Budapest University of Technology and Economics
Faculty of Electrical Engineering and Informatics
Department of Control Engineering and Information Technology

Model reference control of a steer–by–wire steering system

MSc Thesis

Ágoston Lőrincz

2004

Alulírott Lőrincz Ágoston, a Budapesti Műszaki és Gazdaságtudományi Egyetem hallgatója kijelentem, hogy ezen diplomatervet meg nem engedett segítség nélkül, saját magam készítettem, és a diplomatervben csak a megadott forrásokat használtam fel. Minden olyan részt, melyet szó szerint, vagy azonos értelemben, de átfogalmazva más forrásból átvettem, egyértelműen a forrás megadásával megjelöltem.

Tartalmi összefoglaló

A diplomadolgozat egy modellkövető szabályozást ismertet *steer–by–wire* kormányrendszeren. A rendszerkomponensek bemutatása mellett azok jellemző tulajdonságai és a kormányzási mechanizmus működéséhez szükséges szabályozási körök kerülnek bemutatásra.

A modellezési folyamat során a mechanikai alkatrészek fizikai kölcsönhatásait lineáris matematikai módszerekkel írja le. Meggondolások alapján lineáris időinvariáns modelleket állít a folyamatra, és azok paramétereit ARMAX identifikációs módszerrel közelíti.

Az ezt követő fejezetek az identifikált szakasz vizsgálatával, és a modellkövető szabályozás tervezésével foglalkoznak. A követendő linearis modell átviteli függvényeit másoltatjuk le a szabályozóval. Elősször a hagyományos kormányrendszert általános megfontolások alapján [3] másoltuk le. A rendszerre ezután modell követő másodfokú szabályozót terveztünk, majd ennek a rendszernek a kiegészítésével foglalkoztunk adaptív modell követő szabályozásá (MRAC).

Abstract

The present work presents a model following control method for *steer-by-wire* steering system. It contains the representation of the components and explains the characteristic features and control loops generated by the steering mechanisms of the system.

It describes the interactions produced by the physical contact of the mechanical parts with linear mathematical methods. Based upon considerations it follows the process with linear models, and approaches their parameters with ARMAX identification methods.

The last chapters examine the identified system and handle with the planning of a model reference control mechanism. We made the controller copy the transfer functions of the linear model which has to be followed. First we reproduced the conventional steering system based on general considerations. Thereafter, we created a system following two–degree–of–freedom controller, and introduced a model reference adaptive control on its basis.

Ezúton szeretném kifejezni hálás köszönetem Harmati Istánnak és Jánosi Istvánnak folyamatos segítségügért és konzultációs munkájukért. Köszönom Wahl Istvánnak, hogy lehetővé tette az elektromos szervokormány fejlesztésében való részvételem, valamint a ThyssenKrupp Nothelfer Kft Kutató és Fejlesztő Intézetének alkalmazottainak, hogy segítségükkel és tanácsaikkal elősegítették szakmai fejlődésem. Különösen hálás vagyok Szüleimnek tanulmányaim támogatásáért.

I wish to express my sincerest gratitude to István Harmati and István Jánosi for their persistent tutoring and consultation. I thank István Wahl the opportunity to work on electronic steering systems and I also wish to tank all the employees of ThyssenKrupp Nothelfer Research and Development Institute for their help and advices, which ensured my professional development. I am especially grateful to my parents for supporting my studies.

Contents

Chapter 1

Introduction

In next generation vehicles, mechanical and hydraulic subsystems are being replaced by electrical motors and controls. The feature called *drive–by–wire* may include *brake-by-wire* and *steer-by-wire* subsystems, which may boost performance, enhance safety. *Steer–by–wire* offers wide flexibility in the tuning of vehicle handling by software. The lack of steering column makes it possible to design better energy-absorbing structures. The system must be carefully analyzed and verified for safety because it is new and complex. Safety is intimately connected to the notion of risk and popularly means a relatively high degree of freedom from harm.

In steer-by-wire systems the force feedback is necessary, since the *road feel* is one of the most important input for driver, after vision. Force feedback results in the need for large driver forces to steer the system. It is essential for the control strategy to ensure that the force feedback can be adjusted to a comfortable driving environment. An obvious solution is to copy the properties of a conventional hydraulic steering system. This gives a stable system in spite of the uncertain biomechanic dynamics of the driver and vehicle dynamics, that depends on the vehicle iteration with the street.

The goal defined above makes it necessary an exact model of the whole system. If it is not available the *steer–by–wire* system has to be identified. Thus, this *thesis* starts with an ARMAX type identification. Then, a control strategy had been designed based on the general concept of [3]. This controller could not cancel the steady state error caused by uncertainties. Therefore , we created a system following two–degree–of–freedom controller, and introduced a model reference adaptive control on its basis.

Chapter 2

System Description

The purpose of using the *steer–by–wire* steering systems is to make steering more convenient and safe.

The steering system can be divided into three major parts. The first is the hand wheel system, containing the steering wheel, that keeps contact with the driver using an electric motor. An angle sensor provides information about the driver steering input, by resolution 8192 per turn. The steering wheel actuator is accountable for the *road–feel* and for changing the steering dynamics.

The next part is the road wheel system that includes the road wheel actuator, which transmits the steering wheel's angle to the position of the rack. The rotational motion of the motor is converted to translational motion of the rack by a ball-screw drive with a gear of $7 \cdot 10^{-3}$m per turn. An angle sensor gives the motor position to the control, by scaling 4096 per turn. Considering the gear ratio between the rack and the motor it means a resolution of 585143 per meter for the displacement of the rack.

The third part is the *electronic control unit* (ECU). This part has the task to generate the actuator inputs, in the end of view the driver steering input, force feedback, *road–feel*, vehicle and control stability, and importance of safety.

The actuators have additional control loops providing the motor currents by a time constant around 1ms.

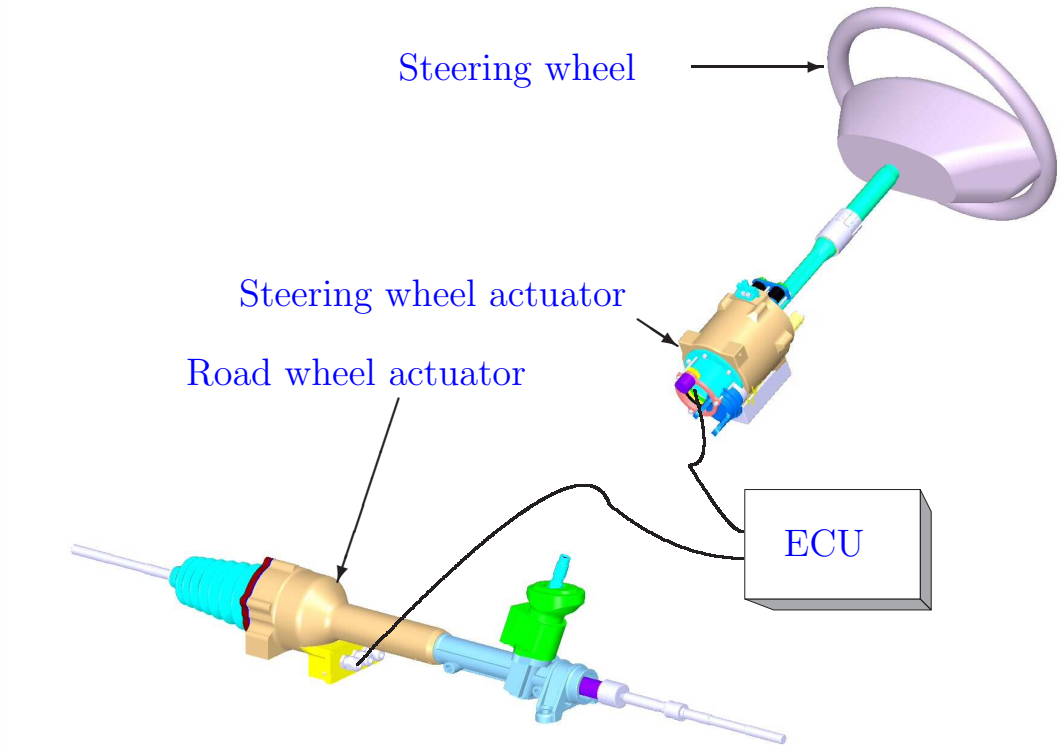

Figure 2.1: Volkswagen steer–by–wire mechanical system

Chapter 3

System Identification

In order to control the system it is necessary to define control outputs, and objectives. In most control systems the object is a physical system, where outputs are significant, observable and usually measurable signals of the system. Inputs are external signals that are possible to be manipulated. The control objective is to follow traces labeled as reference-signals.

So as to design a control for the system it is necessary to assume a relationship between the inputs and outputs [5]. Many systems do not need more than a *mental model*, without any exact mathematical formalization. These systems are usually controlled by human muscle and brain. Several systems can be described by *graphical models*. In many cases at linear models it is sufficient to use their frequency functions, or impulse responses. This model might be the easiest method to describe some non-linearities, too.

In control theory a mathematical model of the system is commonly used for system description. Physical attributes of a system can be described by *ordinary differential equations* or ODEs. It is possible to decompose these higher-order equations into first-order ones. These linear first-order differential equations are often used for process analysis, and are called *state equations*.

In control, linear time-invariant systems are often modeled by their *transfer functions*. Transfer functions are defined as the Laplace transform of the impulse response, with zero valued initial conditions. In systems theory, transfer function is often called the *frequency domain* representation of the system. It describes completely how the system processes the input signals to produce the output signals. Thus, control systems are often designed to meet transfer function specifications. Transfer functions are complex-valued, frequency-dependent quantities, so it is easier to appreciate a systems function by examining the magnitude and phase of its

transfer function. Bode diagrams show magnitude and phase with respect to frequency. Usually they use a logarithmic scale for the frequency, and a decibel scale for the magnitude's great alterations.

Models are constructed from observations. Mental models uses empirical information, graphical models are created from measurements. Analytical model can be developed by stripping it to subsystems are known *a priori*.

There is another way to get mathematical models: some models are based directly on the measurement of the input and output signals of the process. It is necessary to create a particular model structure with several parameters which should be valued during the identification.

In the following section we introduce the mathematical model of the system used for the identification and the results gained with the ARMAX method.

3.1 Mathematical model

The steering system has both mechanical and electrical components as it is showed in Chapter 2. The electrical parts are well known and understood behaviour. It is designed for enlarging robust and allowing fast closed-loop performance, via motor currents. These inner control loops have smaller time constants than the mechanical parts. Therefore we created a model containing only the mechanical subsystems.

The mechanical parts consists of two main parts. The hand wheel system is able to actuate rotational movements, the road wheel system is capable of translational motions. Both systems has only one degree of freedom. Thus, it is possible to describe the systems with a linear model using the Newton's law

$$\sum F = M \cdot \ddot{x} \tag{3.1a}$$

$$\sum T = \Theta \cdot \ddot{\varphi}. \tag{3.1b}$$

Where $\ddot{x}$ is the acceleration. That is the effect of the sum of the forces $\sum F$which are acting on the system's mass M. In a similar way $\ddot{\varphi}$ is the acceleration of the angle φ. This acceleration is caused by the torques acting on the inertia Θ.

Friction

Between moving components and their support devices some friction force occurs. Direction and intensity of this force depends on the two contacting surface, the velocity, the normal force to the velocity, etc. This complex effect has been modeled in various ways.

The most common model describes only the friction force's dependence of the relative speed of the slipping surfaces. This relation is caused by viscous friction. It presumes a linear relation (K) between velocity and friction force (f_v), where (x) is the position of the rack.

$$f_v = -K\dot{x} \tag{3.2}$$

The Coulomb friction does not depend on the amplitude of velocity. It has a constant value (K_c), but the force (f_c) has an opposite direction to the velocity's

$$f_c = -K_c \cdot sign(\dot{x}) = \begin{cases} -K_c \dfrac{\dot{x}}{|\dot{x}|} & \text{if } \dot{x} \neq 0, \\ 0 & \text{if } \dot{x} = 0. \end{cases} \tag{3.3}$$

The whole friction is the sum value of the viscous and the Coulomb friction.

In many cases types of friction modeling mentioned above are not effective, and it is necessary to use more phenomena — like static friction — to get more sufficient results. In our study these friction models gave satisfactory results.

Spring

The identification gave better results when a spring was modeled in the system. The value of the spring force (f_b) and its direction linearly ($-B$) depends on the mass position

$$f_b = -B \cdot x \tag{3.4}$$

3.1.1 Hand wheel system

The mathematical model described above is composed of the moment of inertia, the moment of friction (T_v and T_c), the moment of spring (T_b), the torque developed by driver (T_h), and the actuator torque (τ_{act_h}), as it shown on Figure 3.1. These moments have the directions under the following equation, where (φ) is the steering wheels's angle:

$$-\Theta\ddot{\varphi} + T_h + \tau_{act_h} = T_v + T_c + T_b. \tag{3.5}$$

In this subsystem the equivalent inertia (Θ) of the model contains the inertia of the steering wheel and the inertia of the steering wheel actuator too.

3.1.2 Road wheel system

The road wheel system's mathematical model contains the mass ($M\ddot{x}$), Coulomb (F_c) and viscous (F_v) friction forces, spring force (F_b), the force from the road (*rack force* F_r), and the actuator's force ($F_{act_{Rck}}$) .

$$-M\ddot{x} + F_r + F_{act_{Rck}} = F_v + F_c + F_b, \tag{3.6}$$

The equivalent mass (M) includes the mass of the rack and a reduced mass of the actuator.

During the measurements for the road wheel system's identification, the input was the actuator torque (τ_{Rck}) and the output was the motor angle. Thus, the rack

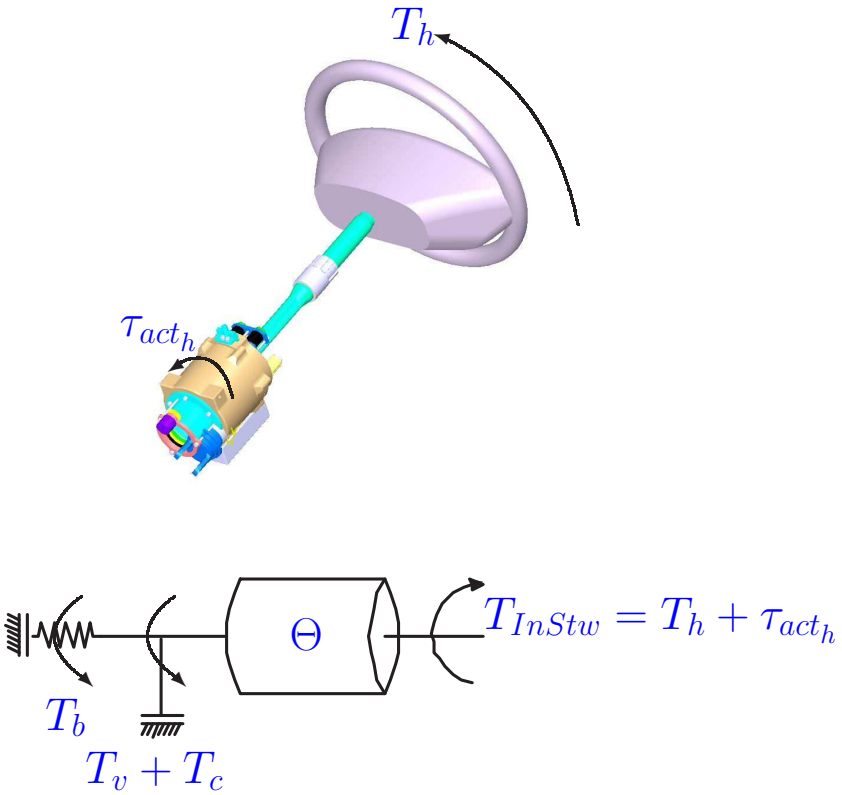

Figure 3.1: Understanding the hand wheel subsystem's mathematical model

forces should be converted into torques on the actuator's mean, the rack motion needs to be transformed to motor angle, see Figure 3.2.

For these calculations there is a linear transformation between x_{Rck} and φ_{Rck}

$$x_{Rck} = i_s \varphi_{Rck}. \tag{3.7}$$

Where i_s is the transmission of the ball-screw drive described in Chapter 2

$$i_s = \frac{7 \cdot 10^{-3}}{2\pi} \frac{m}{rad}. \tag{3.8}$$

Via this transmission all parallel forces actuating on the rack can be transformed into torque with effect on the mean of the motor.

$$T_{Rack} = F_{Rack} \cdot i_s \tag{3.9}$$

The equation (3.9) shows the relation between an arbitrary torque T_{Rack} and the force F_{Rack} belongs to that.

Hence, instead of (3.6) a mathematical model described in the following form will be used for identification.

$$-\Theta_{Rck} \cdot \ddot{\varphi}_{Rck} + T_{Rck} + \tau_{Rck} = T_{v_{Rck}} + T_{c_{Rck}} + T_{b_{Rck}} \tag{3.10}$$

Where Θ_{Rck} is the equivalent inertia of the rack. The actuator's angle is φ_{Rck}, the acceleration of this angle is $\ddot{\varphi}_{Rck}$. The the rack force equivalent torque is T_{Rck}, the actuator torque is τ_{Rck}. The viscous friction torque is $T_{v_{Rck}}$, the Coulomb–friction torque is $T_{c_{Rck}}$, and the spring torque is $T_{b_{Rck}}$.

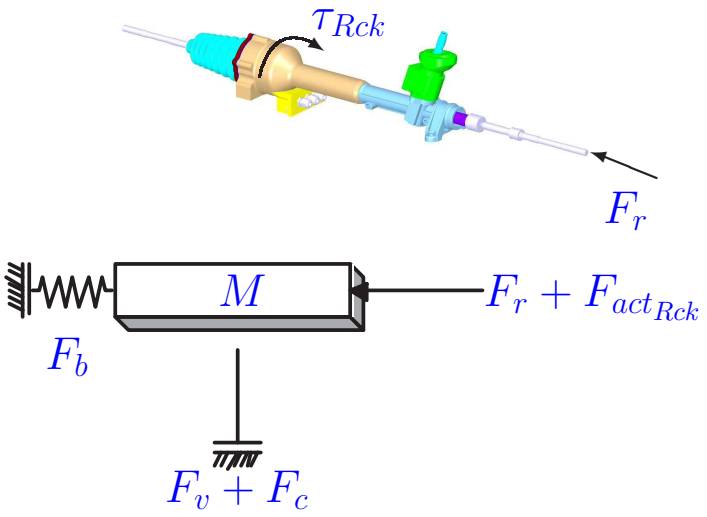

Figure 3.2: Understanding the road wheel subsystem's mathematical model

3.1.3 System Ordinary Differential Equations

Inasmuch as the forces acting in the system are known, it is possible to create the system ODEs to see the dynamics in an analytical form.

$$\tau_{act_h} + T_h = \Theta\ddot{\varphi} + K_{Stw}\dot{\varphi} + K_{cStw}sign(\dot{\varphi}) + B_{Stw}\varphi \tag{3.11a}$$

$$\tau_{Rck} + T_{Rck} = \Theta_{Rck}\ddot{\varphi}_{Rck} + K_{Rck}\dot{\varphi}_{Rck} + K_{cRck}sign(\dot{\varphi}_{Rck}) + B_{Rck}\varphi \tag{3.11b}$$

Where $\dot{\varphi}_{Rck}$ is the velocity of rack actuator angle, and similarly $\dot{\varphi}_{Stw}$ is the velocity of the steering wheel angle. The Coulomb–frictions are represented as K_{cStw} on the steering wheel subsystem, and K_{cRck} on the road wheel subsystem. Similarly K_{Stw} is the viscous friction on steering wheel subsystem and K_{Rck} is the viscous friction on road wheel subsystem. The spring is modeled by B_{Stw} and B_{Rck}.

Both subsystems have two inputs, one external torque — the driver on the steering wheel subsystem and the wheel load on the road wheel subsystem— and

one applied actuator torque. The two torques effect the same inertia therefore one can define T_{InStw} and T_{InRck} as the sum of system inputs.

$$T_{InStw} = \tau_{act_h} + T_h \tag{3.12a}$$

$$T_{InRck} = \tau_{Rck} + T_{Rck} \tag{3.12b}$$

It is important for control, that there is only one controllable input in both subsystems. The T_{Rck} and T_h signals are not controllable, but they are reference signals.

Transfer functions (S_h ,W_{Rck}) can be reached by Laplace transforming equations (3.11) with the negligence of the Coulomb friction. The transfer function S_r describes the system with T_{InStw} input, and angle output. Transfer function W_{Rck} has T_{InRck} input, and motor angle output. The road wheel subsystem's equation contains another transfer function S_R, that is describing the subsystem using force input and position output.

$$S_h(s) = \frac{\varphi}{T_{InStw}} = \frac{1}{\Theta s^2 + K_{Stw}s + B_{Stw}} \tag{3.13a}$$

$$W_{Rck} = S_R(s) \cdot i_S = \frac{\varphi_{Rck}}{T_{InRck}} = \frac{1}{\Theta_{Rck} s^2 + K_{Rck}s + B_{Rck}} \tag{3.13b}$$

In cognition of $S_h(s)$ and $S_R(s)$ it is possible to describe the system in the following form, that is based on equations (3.12) and (3.13). That is an appropriate description showing the architecture of the steer–by–wire system.

$$\varphi = S_h(s)\left(T_h + \tau_{act_h}\right) \tag{3.14a}$$

$$x = S_R(s)\left(\frac{\tau_{Rck}}{i_S} + F_r\right) \tag{3.14b}$$

3.2 ARMAX Model

To identify the system it is possible to adapt an identification model structure to the given system, which parameters should be estimated. Parameter identification uses measurements about the given system. As the driver torque is not measurable at the steering wheel subsystem, for these measurements only the actuator's input has effects on the system. At the road wheel subsystem, the rack force is not measurable, so only the motor activates the system during the measurements. In order to improve the identification a noise model is implemented in the system. To have freedom in describing the term of the disturbance, an auto regressive with moving average exogenous signal (ARMAX) structure is chosen.

$$y(t) = \frac{B(q)}{A(q)}u(t) + \frac{C(q)}{A(q)}e(t) \tag{3.15}$$

If model is described in the

$$y(k) = G(q)u(k) + H(q)e(k) \tag{3.16}$$

form, then prediction error method used for parameter identification[1] is:

$$\varepsilon(k) = H^{-1}(q)[y(k) - G(q)u(k)]. \tag{3.17}$$

Where $G(q) = \dfrac{B(q)}{A(q)}$ and $H(q) = \dfrac{C(q)}{A(q)}$. Thus, different identification structures results different loss function values.

The loss function is defined

$$\begin{aligned} E[y(k+l) - \hat{y}]^2 =& E[H_l(q)e(k+l)]^2 + E\left\{G(q)u(k+l)\right\}^2 + \\ &+ E\left\{\tilde{H}_l(q)H^{-1}(q)[y(k) - G(q)u(k)] - \hat{y}\right\}^2 \longrightarrow min \end{aligned} \tag{3.18}$$

One can see that the value of the loss function depends on the model type as much as the model parameters. This means that different model structure or different dimensions may result absonant loss function value, even the smaller value not results the better parameters.

At ARMAX structure the prediction error characteristic can be described by

[1]The loss function description and its use are based on [1] and [6].

$$\vartheta = \begin{bmatrix} a_1 & a_2 \dots a_{n_a} & b_1 & b_2 \dots b_{n_b} & c_1 & c_2 \dots c_{n_c} \end{bmatrix}^T \tag{3.19a}$$

$$V_N(\vartheta, Z^N) = \frac{1}{N} \sum_{t=1}^{N} \frac{1}{2} |\varepsilon_F(t, \vartheta)|^2 \tag{3.19b}$$

$$V_N^{'}(\vartheta, Z^N) = -\frac{1}{N} \sum_{t=1}^{N} \Psi(t, \vartheta) \varepsilon_F(t, \vartheta), \tag{3.19c}$$

where ϑ is a raw vector containing the actual parameter values. We can define the first derivative of ε by ϑ as $-\Psi(t, \vartheta)$. Thus, it is possible to define $V_N^{'}(\vartheta, Z^N)$ as the first derivative of the error characteristic.

$$V_N^{''}(\vartheta, Z^N) = \frac{1}{N} \sum_{t=1}^{N} \Psi(t, \vartheta) \Psi^T(t, \vartheta) \tag{3.20}$$

Where $V_N^{''}(\vartheta, Z^N)$ is called Hess-matrix. This allows to use the quasi-Newton formula, that usually establishes a good and fast convergence. Ψ is described as:

$$\Psi(t) = \frac{1}{C(q)} \cdot \\ \cdot \begin{bmatrix} -y(t-1) \cdots - y(t-n_a) & u(t) \dots u(t-n_b+1) & \varepsilon(t-1) \dots \varepsilon(t-n_c) \end{bmatrix}^T \tag{3.21}$$

The first step of the identification is to measure the input and output signals. It was not possible to carry out new measurements, only to use existing data. At these measurement inputs were sinusoid signals with different amplitude and frequency, with the sample time $T = 10^{-3}s$. Both frequency and amplitude have limitations based on the physical constraints, for example backstop. The small amplitude causes little velocity, and it highlights the friction non-linearities, so we neglected the measurements which were hazardous in the aspect of this effect. Another disadvantage of the existing measurements is that we are not able to make data sets for special examination of a parameter. It is an easy way to determine the value of Coulomb–friction by measuring the input value when the position starts changing, but in this case we had to find another way to reach this parameter.

The models resulted from the identification were simulated with the measured input, which was used for the identification itself. This way one could compare the parameters of the measured outputs, and the simulation results, the outputs' fit. Thus, it is possible to classify identified parameters by the loss function, and simulation results, too.

It is important to chose the model's dimensions. At ARMAX model three dimension is have to be defined, the polynomial order of the polynomial $A(q)$ is n_a, the polynomial order of $B(q)$ is n_b, and $C(q)$ has polynomial order n_c. Proceeding equations (3.13) the ARMAX model dimensions were chosen as $n_a = 2$ and $n_b = 1$. In order to identify the polynomial order of the moving average noise more values were tried. We had to examine this dimension influence on the outputs' fit. Small dimensions had not resulted adequate fit, so a value $n_c = 10$ was chosen for both the steering wheel and the road wheel subsystems. The necessity of this accurate disturbance model shows, that the systems have bad signal-to-noise ratios, or their non-linearity is big.

Let us estimate the Coulomb–friction next. Coulomb–friction is realizable as an additive torque on the system. One can reduce it from the measured inputs using a simple subtraction. As the interpretable model structure is not changing, the best Coulomb–friction value causes the smallest loss function value as it described in equation (3.18). If one summarizes the loss function values resulted from a given value of the Coulomb–friction on all measurement of the given system, the result is a value that shows a type of goodness of the Coulomb–friction value. One can determine the value resulting the smallest summation by using the MATLAB's *fminsearch* [4] command. This function is able to find a minimum of a scalar function of several variables. It uses a simplex algorithm that does not depend on the gradient, it changes the values directly, and keeps the resulting smaller value on the scalar function. The loss function's sum as the scalar function resulted different minimums at variant initial states. Presumably the function finds a local minimum point — that depends on initial values — and stops there. Hence the function resulting the loss functions' sum has run in a wide range of Coulomb–friction values. One can plot the resulting values as the function of the Coulomb-friction. It is possible to find the minimum of the loss function on that figure, and to get the Coulomb–friction which belongs to that.

The second method represents the Coulomb–friction's work on the loss function value. Several noise-like jump can be observed on Figures 3.3 and 3.4, so a value consisting of the normal course had been chosen. The value on the road wheel subsystem is greater than on the steering wheel subsystem, it is caused by the greater forces, and mass.

$$K_{CoulombStw} = 0.192Nm \tag{3.22a}$$

$$K_{CoulombRck\theta} = 0.368Nm \tag{3.22b}$$

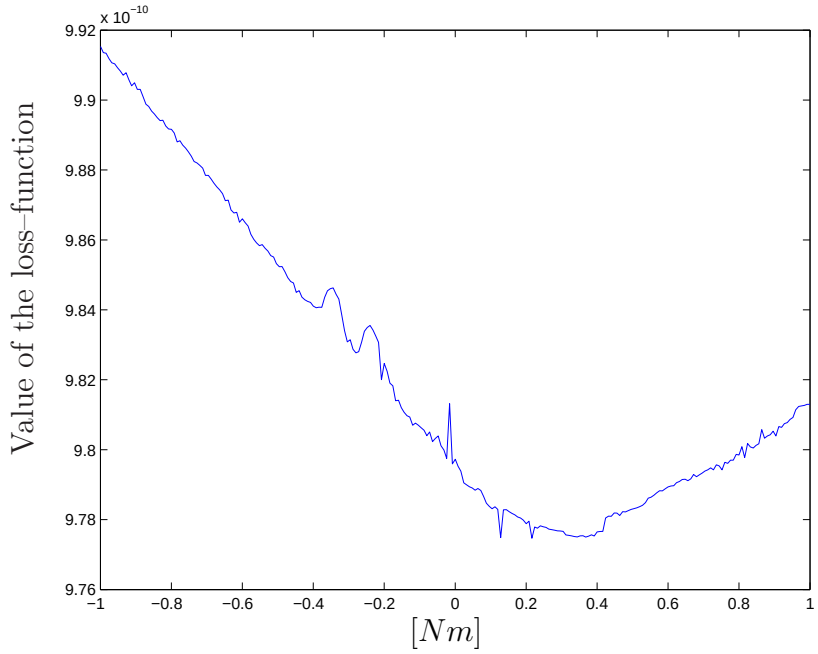

Figure 3.3: Loss-function final values based on Road-wheel Coulomb–friction

As there are more measurements for each subsystems, the linear transfer functions — obtained from the ARMAX method, feed–forwarding the identified Coulomb–friction values — are not the same. Presumably this effect is caused by other non-linearities. Like by the estimation of the Coulomb–friction the decision between these models based on error minimizing. Thus, the task is to choose the model which causes the smallest error covariance under all measured data for that subsystem. Hence, these models have been used to describe the system, and control developing had been based on these models, too.

Steering wheel

The above identified discrete time transfer function is:

$$S_{hDiscrete} = \frac{2.605 \cdot 10^{-5}}{z^2 - 1.9988z + 0.9988} \tag{3.23}$$

The transfer functions derived from the identification of other measurements had parameter differences in the values' last two decimals.

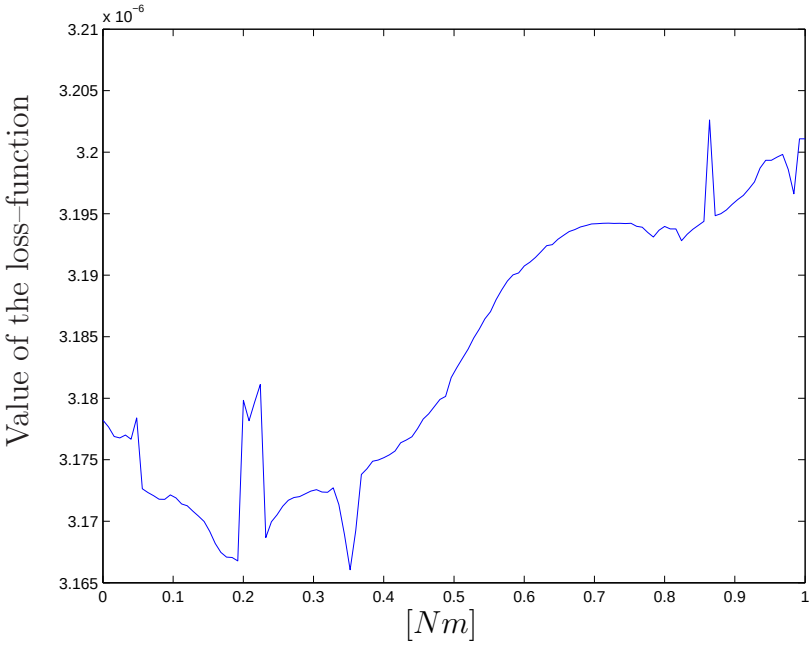

Figure 3.4: Loss-function final values based on Steering-wheel Coulomb–friction

This transfer function can be transformed to continuous time. Assuming zero order hold on its input, the transformation only bases on $z = e^{-sT}$, and can be computed by the MATLAB's *d2c* command. The zero order hold inserts a zero in the continuous time transfer function compared to (3.13). The polynomial element $-0.01303 \cdot s$ on the numerator of the continuous time, can be neglected, because of its small value.

$$S_h = \frac{-0.01303s + 2.606}{s^2 + 1.153s + 0.0567} \tag{3.24}$$

Thus, from equation (3.13) and (3.24) parameters introduced in section 3.1 are able to be assigned.

$$\Theta = 0.0384 kgm^2$$

$$K_{Stw} = 0.0443 \frac{Nms}{rad} \tag{3.25}$$

$$B_{Stw} = 0.0022 Nm$$

Rack

The discrete time transfer function for the road wheel subsystem identified by the ARMAX method is described in equation

$$W_{RckDiscrete} = \frac{6.613 \cdot 10^{-7}}{z^2 - 1.9922z + 0.9922}. \tag{3.26}$$

The transfer functions derived from the identification of other measurements had parameter differences in the values' last two decimals.

Analogous to steering wheel subsystem, this transfer function can be transformed to continuous time. The continuous transfer function

$$W_{Rck} = \frac{-0.0003s + 0.6639}{s^2 + 7.861s + 0.8585} \tag{3.27}$$

describes the system's dynamics between the actuator's torque and the motor angle. To get the equivalent rack mass, it is necessary to convert the transfer function input into force and output into position. This force-to-position transfer function contains the parameters have been shown in section 3.1

$$M = 1352kg$$

$$K_{xRck} = 10629\frac{Ns}{m} \tag{3.28}$$

$$B_{xRck} = 1161\frac{N}{m}$$

The big value of the mass is caused the reduced motor inertia.

The Coulomb–friction's value has to be converted to attain a full set of parameters about the forces actuating the road wheel subsystem.

$$K_{xcRck} = 330.316\frac{Ns}{m} \tag{3.29}$$

3.3 Simulink model of the system

Using Simulink environment to examine the identified steer–by–wire system's ability, it is important to create a Simulink model.

The easiest method for modeling the system is the usage of continuous transfer function blocks. It is possible to describe the whole system with two transfer function blocks. This architecture makes impossible to examine all signals, such as the velocity of the rack's position, or the value of the friction force.

In this case it is recommended to use another block diagram, that relies on the ordinary differential equations of the system. The model's input (see on Figure 3.5) is the superposition of the external forces, for example at the steering wheel subsystem it is T_{InStw} see equations (3.12). This force is reduced with the friction force and the spring force. Consequently, it equals numerically to the product of the mass and the acceleration. Thus, the output of the system is the second integral of the acceleration, that is the position. All other signals modeled in section 3.1 are possible to be measured. For example the friction force can be measured after the light blue gain block, K.

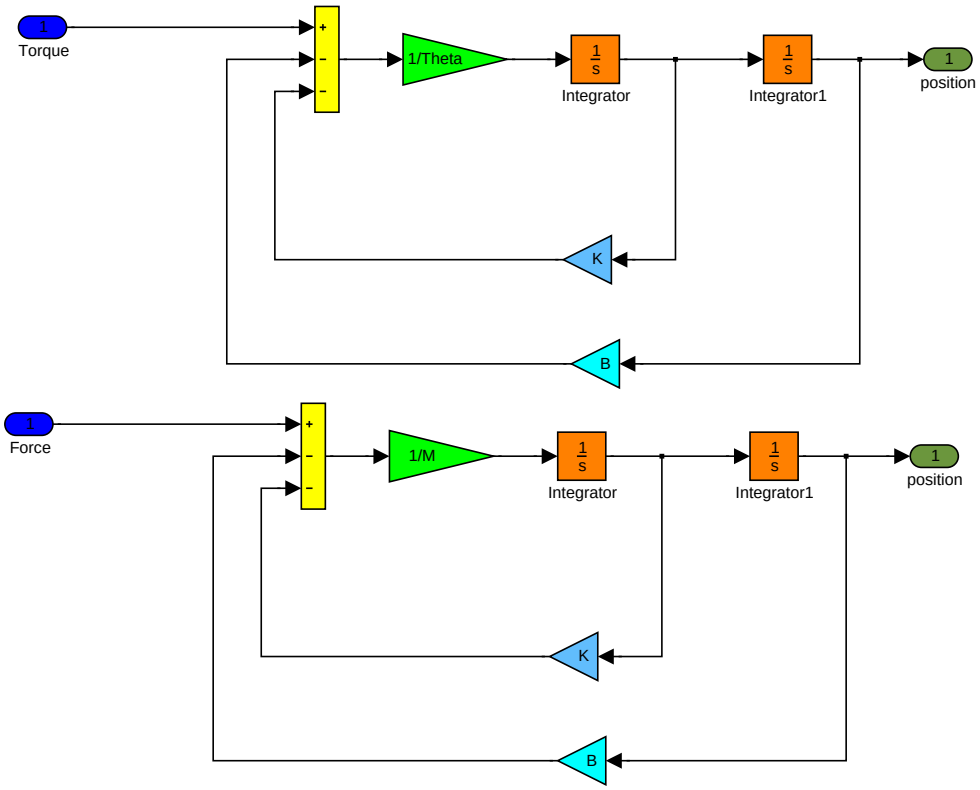

Figure 3.5: Create steer–by–wire model in Simulink environment

Chapter 4

Model Reference Control

As it have been indicated in section 1, simple force feedback requires excessing torque from the driver, so it is important — in the aspect of choosing the control structure — to create the possibility of decreasing the driver's torque. Another problem is— as a common requirement for control — that the system must be stable despite of the uncertain biomechanical dynamics of the driver, or uncertain vehicle dynamics. An obvious solution is to copy the properties of a conventional steering system. This conventional steering system might be a mechanical steering system without power assistance, or a modern car, with hydraulic power assistance (HPAS), electro–hydraulic power assistance (EHPAS), or electric power assistance (EPAS). The whole system can be divided into two parts from the control's point of view. The first part is the manual steering, which can be approximately described with a linear model. The other part, the power steering part is generally non-linear. This subsystem is missing at mechanical steering systems.

The proposition is to copy the dynamics of another system means, that all dynamics of the steer–by–wire systems may be change. This might allow to the driver to adjust the dynamics, even the power assist to its condition, driving habits or to the weather conditions, making the steering more comfortable, safe and enjoyable.

The following section first introduces the power assisted steering system model, and describes the three control methods developed in the diploma.

4.1 Power Assisted Steering System

In order to create a control over the steer–by–wire system which copies the dynamics of a power steering system, it is inevitable to know a mathematical model about that. In this thesis the power assisted steering system (power system) model is divided into three parts.

The first part — like at the steer–by–wire system — is the steering wheel part. Its dynamics are described by a moment of inertia, and friction moment. The external forces acting in this part are the driver torque and another torque from the torsion bar.

The second part is the torsion bar, that accomplishes force and position relationship between steering wheel, and road wheel subsystems. In reality this spring has end–stops to prevent the torsion bar from irreversible deformations, so it can usually not be modeled by linear characteristic, but only big external torque enable to the spring to reach this external frame, so we mostly used a linear spring model for it

$$T_{TS} = P_P(s)\left(\varphi_{PS} - \frac{x_r}{i_P}\right), \tag{4.1}$$

where $P_P(s)$ is a constant in linear cases. Another constant in this equation is i_p, that is the transmission constant between rack and steering column.

$$i_P = \frac{0.05047}{2\pi}\frac{m}{rad} \tag{4.2}$$

The third part is the road wheel subsystem. Like the steering wheel subsystem in the power system, it is modeled by a mass and friction. It has actuating forces from the torsion bar, from the road, and — if it is not a model of a mechanical steering — there is the assist force $F_{a,PS}$, that usually acts on the rack.

Now, the power system can be described with the following mathematical model:

$$\varphi_{PS} = P_h(s)\left(T_h - T_{TS}\right) \tag{4.3}$$

$$x_{rPS} = P_R(s)\left(\frac{T_{TS}}{i_P} + F_{a,PS} + F_r\right). \tag{4.4}$$

T_{TS} is the torsion bar's torque, it has an opposite direction to the driver's torque. P_h is a transfer function from torque to angle on the steering wheel subsystem, P_R is a transfer function from force to position on the road wheel subsystem.

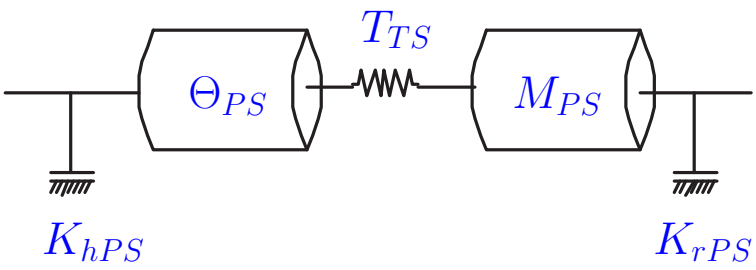

Figure 4.1: Power system's mathematical model

The power system's exact values, and P_h, P_R transfer functions are described in the following equations

$$P_h = \frac{1}{\Theta_{PS} \cdot s^2 + K_{hPS} \cdot s} = \frac{22.22}{s^2 + 0.2222 \cdot s} \tag{4.5}$$

$$P_R = \frac{1}{M_{PS} \cdot s^2 + K_{rPS} \cdot s} = \frac{0.0007143}{s^2 + 0.001357 \cdot s} \tag{4.6}$$

$$P_P = 91.67 \frac{Nm}{rad} \tag{4.7}$$

4.2 Concept of making steer–by–wire feeling

We follow the concept of [3] to copy the properties of a conventional steering system, which means the equivalence of positions and forces between steering wheel and road wheel subsystems in both directions. This equivalence might be mathematically reached, if the equivalence of both external inputs — the τ_{act_h} and τ_{Rck} — call forth equivalence of rack position and steering wheel angle.

Thus, one can evaluate from equations (4.1) – (4.4) for the power system:

$$T_h = \varphi_{PS}\left(\frac{1}{P_h} + P_P\right) - x_r\frac{P_P}{i_P} \tag{4.8a}$$

$$F_r = x_{rPS}\left(\frac{1}{P_R} + \frac{P_P}{{i_P}^2}\right) - \frac{P_P}{i_P}\varphi_{PS} - F_a. \tag{4.8b}$$

Assimilating the steer–by–wire system with the power system, the actuator's torque has to simulate the torque from the spring. Another task of each actuator is to change the given subsystem's dynamics to the copied conventional system's dynamics, and the road wheel actuator already has the same objective as on the power system to generate the assist force. Thus, the torque of the steering wheel actuator depends on the steering wheel angle — torque for changing the dynamics — and rack position — torque of the torsion bar. Similarly, the torque of the road wheel actuator depends on the steering wheel angle — torque of the torsion bar — and rack position — torque for changing the dynamics. The superposition of these torques gives the steer–by–wire actuators torque:

$$\begin{bmatrix}\tau_{act_h}\\ \tau_{Rck}\end{bmatrix} = \begin{bmatrix}C_{11} & C_{12}\\ C_{21} & C_{22}\end{bmatrix}\begin{bmatrix}\varphi\\ x\end{bmatrix} + \begin{bmatrix}0\\ C_{25}\end{bmatrix}F_a \tag{4.9}$$

Where C_{xy} is a transfer function between position and requested torque.

In order to reach the equivalence of the two systems, these C_{xy} functions should be determined. The problem can be resolved by transforming the steer–by–wire equations (3.14) and (4.9) into a form similar to the power system's equation (4.8), where S_h and S_r are the identified steering system's transfer functions.

$$T_h = \varphi\left(\frac{1}{S_h} + C_{11}\right) + C_{12}x_r \tag{4.10a}$$

$$F_r = x\left(\frac{1}{S_R} - \frac{C_{22}}{i_S}\right) - \frac{1}{i_S}\left(\varphi C_{21} + C_{25}F_a\right) \tag{4.10b}$$

Making equations (4.8) and (4.10) equal the functions which ensure that the systems' equality can be accomplished:

$$C_{11} = P_P + \frac{1}{P_h} - \frac{1}{S_h} = \tag{4.11a}$$
$$= \frac{3.84s^2 - 19.84s + 5.309 \cdot 10^4}{579.2}$$
$$C_{12} = -\frac{P_P}{i_P S} = -1.141 \cdot 10^4 \tag{4.11b}$$
$$C_{21} = \frac{i_S P_P}{i_P} = 12.71 \tag{4.11c}$$
$$C_{22} = -\frac{i_S P_P}{{i_P}^2} + i_S \left(\frac{P_R - S_R}{P_R S_R} \right) = \tag{4.11d}$$
$$= \frac{-4.101 \cdot 10^{-12} s^2 + 6.477 \cdot 10^{-6} s - 0.0008653}{5.471 \cdot 10^{-7}}$$
$$C_{25} = i_S = 1.114 \cdot 10^{-3} \tag{4.11e}$$

Since C_{11} and C_{22} have larger dimensions on their numerator than on their denumerator, these transfer functions are acausals, that means that the signal values from the future are used for computing the output. According to [3] it is possible to solve this problem by inserting a second order low–pass filter with transfer function, where $\xi = 1$ and $T = (2\pi 500)^{-1}$:

$$W_{LowPass} = \frac{1}{T^2 s^2 + T\xi s + 1} = \frac{1}{1.013e \cdot 10^{-7} s^2 + 0.0003183 s + 1} \tag{4.12}$$

According to the previous discussion, four transfer functions can exactly determine the power system. One of these transfer functions converts the driver's torque to steering wheel's angle (P_{11}), the other one is the transfer function that converts the driver's torque to rack position (P_{12}). There are two transfer functions that describe the effects of the rack force, one of them actuates the rack itself (P_{22}), and the other one effects on the steering wheel (P_{21}). An additional transfer function should be added to this system to describe the effect of the assist force on the rack. Thus, equation

$$\begin{bmatrix} \varphi \\ x \end{bmatrix} = \begin{bmatrix} P_{11} & P_{21} \\ P_{12} & P_{22} \end{bmatrix} \begin{bmatrix} T_h \\ F_r \end{bmatrix} + \begin{bmatrix} 0 \\ P_{23} \end{bmatrix} F_a \tag{4.13}$$

can describe the complete power steering system. The steer–by–wire control described above can be rated, if the power system's transfer functions can be corresponded — with the same inputs and outputs — to the ones of steer–by–wire system.

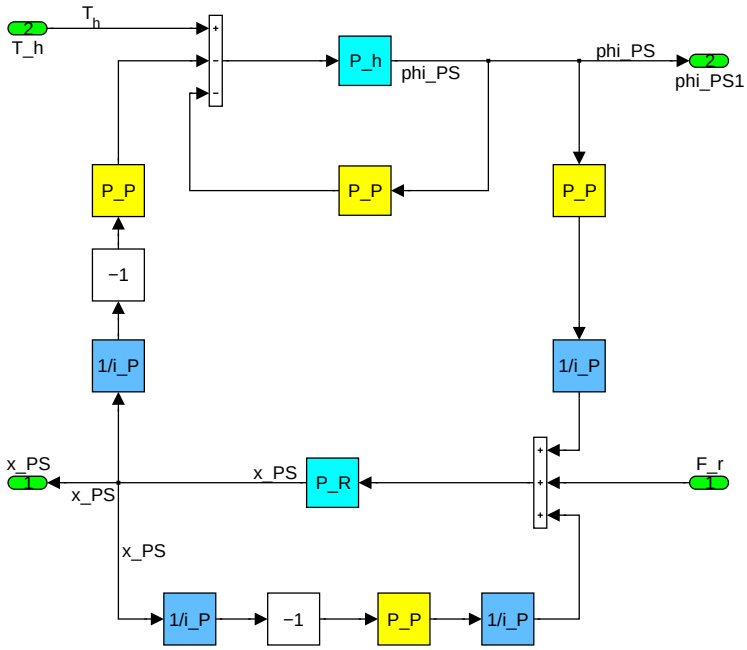

Figure 4.2: The power system model in MATLAB Simulink environment

Figure 4.2 shows the power system's block–diagram. Using this figure it is possible to create P_{io} (input-output) transfer functions.

As figure shows, both subsystems have two feedbacks, one is across the torsion bar (P_P) to itself, and a second one across the other subsystem — with the other subsystem's first feedback — and the torsion bar. The block–diagram becomes simpler if this first feedback integrated into the system blocks, as it follows

$$P_{hB} = \frac{P_h}{1 + P_h \cdot P_P} \tag{4.14a}$$

$$P_{RB} = \frac{P_R}{1 + \dfrac{P_R \cdot P_P}{{i_P}^2}}. \tag{4.14b}$$

Thus, P_{hB} describes a system with driver torque input, steering wheel output across P_h, and a negative feedback P_P. Similarly to this P_{RB} describes a system with input rack force, output rack position, across P_R, and negative feedback $P_P/{i_P}^2$.

Using these simplifications on the transfer functions for equation (4.13) we get:

$$P_{11} = \frac{P_{hB}}{1 - \frac{P_{hB} \cdot P_P^2 \cdot P_{RB}}{{i_P}^2}} = \frac{22.22s^2 + 0.03123s + 23350}{s^4 + 0.2263s^3 + 3088s^2 + 236.4s} \tag{4.15a}$$

$$P_{12} = \frac{\frac{P_{hB} \cdot P_P \cdot P_{RB}}{i_P}}{1 - \frac{P_{hB} \cdot P_P^2 \cdot P_{RB}}{{i_P}^2}} = \frac{187.6}{s^4 + 0.2236s^3 + 3088s^2 + 236.4s} \tag{4.15b}$$

$$P_{21} = \frac{\frac{P_{hB} \cdot P_P \cdot P_{RB}}{i_P}}{1 - \frac{P_{hB} \cdot P_P^2 \cdot P_{RB}}{{i_P}^2}} = \frac{187.6}{s^4 + 0.2236s^3 + 3088s^2 + 236.4s} \tag{4.15c}$$

$$P_{22} = \frac{-P_{RB}}{1 - \frac{P_{hB} \cdot P_P^2 \cdot P_{RB}}{{i_P}^2}} == \frac{-0.0007396s^2 - 0.0001644s - 1.507}{s^4 + 0.2236s^3 + 3088s^2 + 236.4s} \tag{4.15d}$$

Figure 4.3 shows the steer–by–wire system's block–diagram.

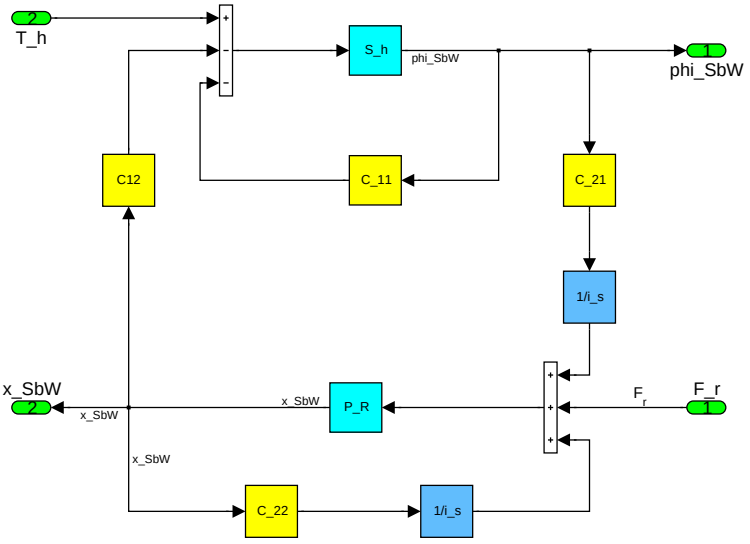

Figure 4.3: The steer–by–wire system model in MATLAB Simulink environment

One can see, the necessary cross–activity is solved by the C_{xy} functions, and this way a matrix–equation similar to (4.13) can be processed.

$$\begin{bmatrix} \varphi \\ x \end{bmatrix} = \begin{bmatrix} S_{11} & S_{12} \\ S_{21} & S_{22} \end{bmatrix} \begin{bmatrix} T_h \\ F_r \end{bmatrix} + \begin{bmatrix} 0 \\ S_{23} \end{bmatrix} F_a \tag{4.16}$$

Similarly to power system's transfer functions this figure might be reduced by defining inner feedbacks. The inner feedbacks contain the C_{11} or C_{22} transfer functions:

$$S_{hB} = \frac{S_h}{1 + S_h \cdot C_{11}} \tag{4.17a}$$

$$S_{RB} = \frac{S_R}{1 + \dfrac{S_R \cdot C_{22}}{i_s}} \tag{4.17b}$$

Where S_h and S_R transfer functions are identified in section 3.2.

Based on the short-circuit block–diagram the transfer functions S_{io} were possible to be counted in the form:

$$S_{11} = \frac{S_{hB}}{1 + \dfrac{S_{hB} \cdot C_{12} \cdot S_{RB} \cdot C_{21}}{i_s}} \tag{4.18a}$$

$$S_{12} = \frac{-S_{hB} \cdot C_{12} \cdot S_{RB}}{1 + \dfrac{S_{hB} \cdot C_{12} \cdot S_{RB} \cdot C_{21}}{i_s}} \tag{4.18b}$$

$$S_{21} = \frac{\dfrac{S_{hB} \cdot C_{21} \cdot S_{RB}}{i_s}}{1 + \dfrac{S_{hB} \cdot C_{12} \cdot S_{RB} \cdot C_{21}}{i_s}} \tag{4.18c}$$

$$S_{22} = \frac{-S_{RB}}{1 + \dfrac{S_{hB} \cdot C_{12} \cdot S_{RB} \cdot C_{21}}{i_s}} \tag{4.18d}$$

The equality of the assist forces depends on another effect. Especially, the assist force of the power system is —as described above —a generically non-linear function. Its variables might be for example the torque of the torsion bar, the steering wheel's angle and the vehicle speed. All the signals it uses as variables are measurable on the steer–by–wire system, or they appear on the outputs of the C_{12} and C_{21} transfer functions, so S_{23} needs to be equal to P_{23} in order to copy the power system's characteristics.

Now, all transfer functions of the two linear systems — the power steering system and the steer–by–wire system — are known. With drawing the Bode-plots of compounding transfer functions, it is possible to get information about the similarity of the two systems.

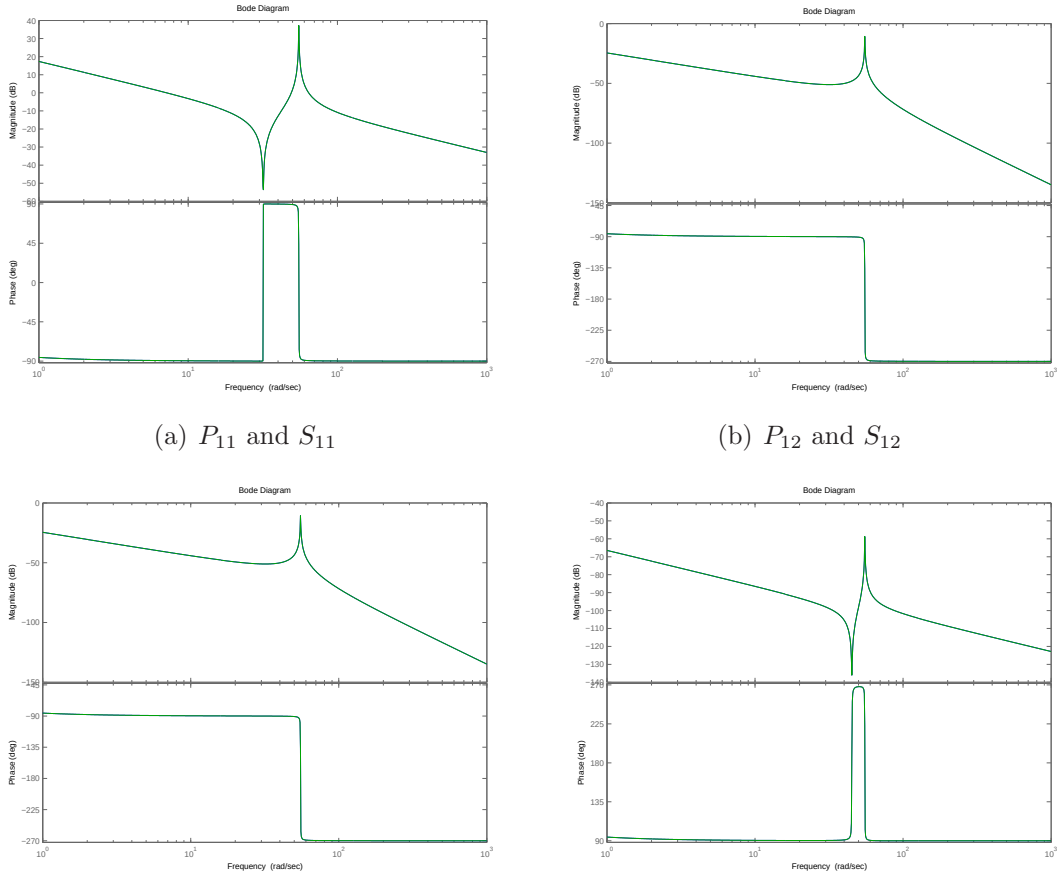

(a) P_{11} and S_{11}

(b) P_{12} and S_{12}

(c) P_{21} and S_{21}

(d) P_{22} and S_{22}

Figure 4.4: Compare the Bode-diagram of compounding transfer functions

As it can be seen on Figure 4.4 in frequency domain the compounding transfer functions are the same in the examined range, that encompasses the interval of the usual driving. In MATLAB Simulink environment it is possible to test the two systems. To examine the equality of the power system, and the steer–by–wire system, both systems are driven by the same driver (the Simulink block diagram is illustrated on Figure 4.6). The driver is modeled with a PID controller, that has the transfer function W_{PID}.

$$W_{PID} = 501 + \frac{500}{s} + 1s \tag{4.19}$$

Both of the PID controllers have got the same reference signal for steering wheel's angle. The measured signals are the angle, the rack's position, and the driver's torque to test the feeling equality. The results — are shown in Figure 4.5 — show small difference between the conventional steering system and steer–by–wire system.

In section 3.2 it was shown, that the not modeled non-linearities can cause uncertainty in the steer–by–wire system's parameters. These uncertainties might cause

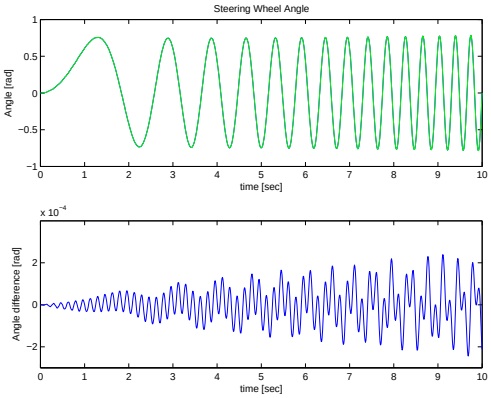

(a) The steering wheel angles

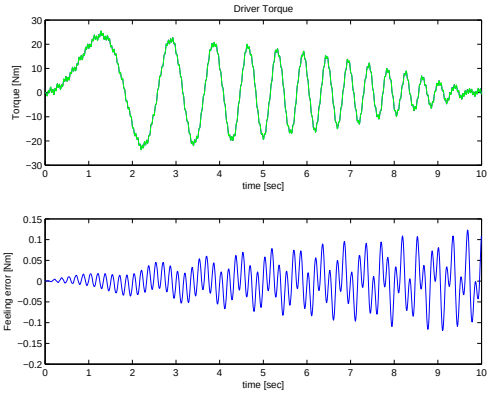

(b) The driver's torques

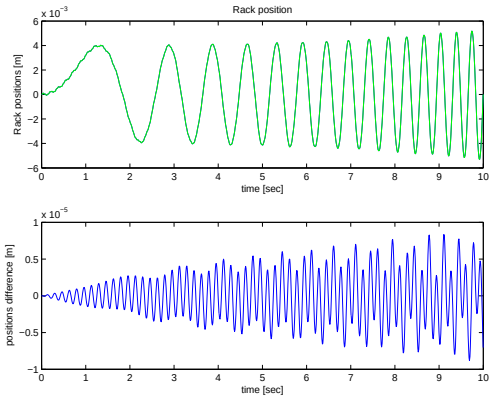

(c) The rack's positions

Figure 4.5: Compare the power system and the steer–by–wire system

steady state error in the feeling. The control designed above has not got the ability to eliminate this error. It is usual to examine the effected parameter fluctuations by changing the system's parameters manually by $\pm 25\%$ of its values in the simulation, but using the original controller designed for nominal system. Transfer functions for Bode-plots can be computed by using C_{xy} for the original system, and the other transfer functions in steer–by–wire system are used with the changed parameters.

Decreasing parameters by 25% cause a positive offset on the system's Bode–plot, and it increases the feeling error as well as the steering wheel position and the rack position does not match the values on the power system.

As it was shown in this section this control strategy ensures a high level of equivalence while the system parameters have no uncertainty.

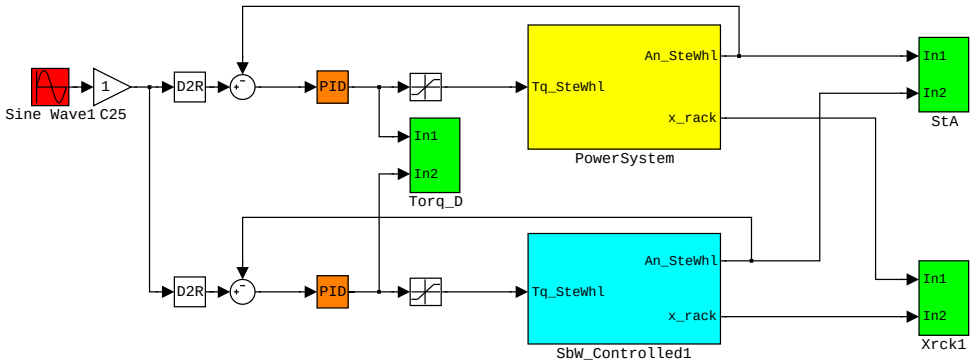

Figure 4.6: The Simulink environment block diagram testing the equality

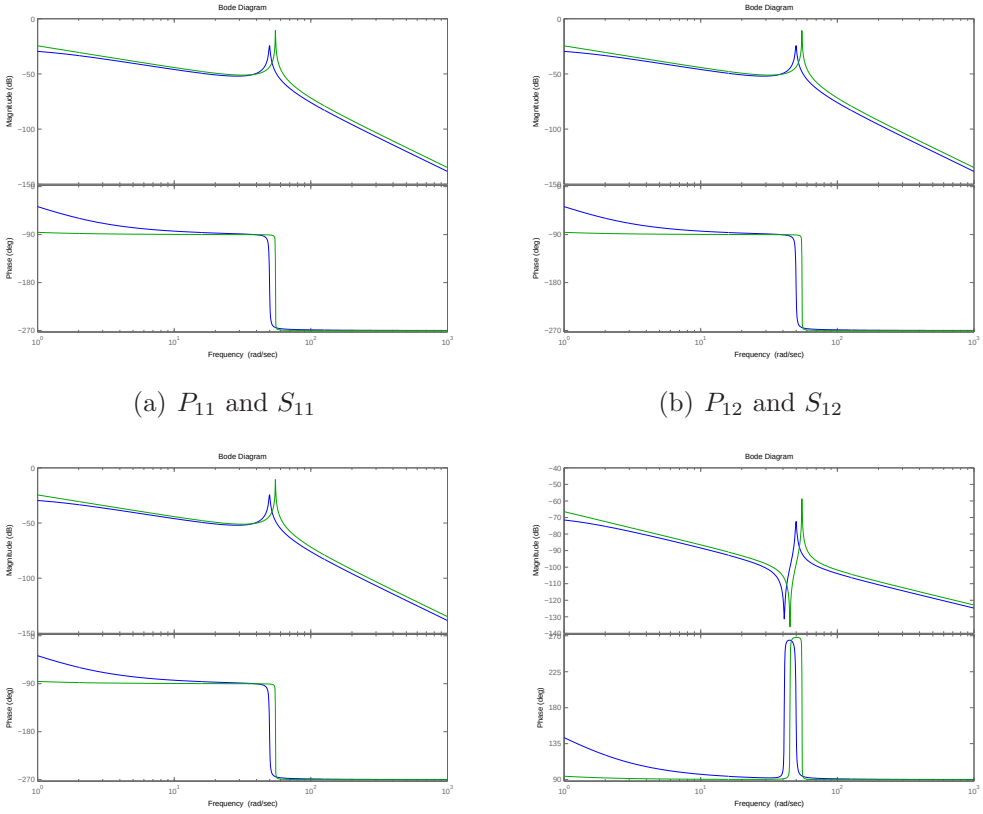

(a) P_{11} and S_{11}

(b) P_{12} and S_{12}

(c) P_{21} and S_{21}

(d) P_{22} and S_{22}

Figure 4.7:
Bode-diagrams of power system's (blue) and steer–by–wire system's (green) if system parameters are reduced by 25%

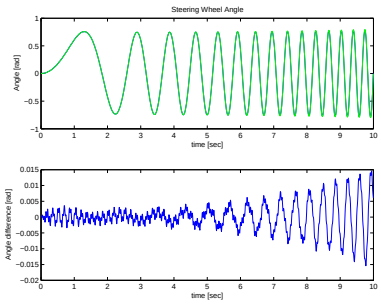

(a) The steering wheel angles

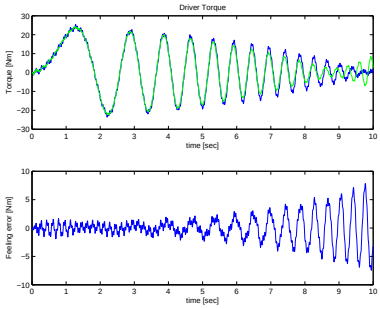

(b) The driver's torques

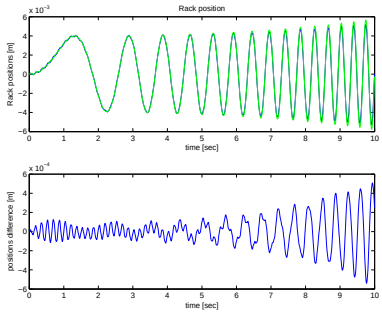

(c) The rack's positions

Figure 4.8:
Compare the power system (blue) and the steer–by–wire system (green) if system parameters are reduced by 25%

4.3 Model reference controller

As it was stated in section 4.2, the linear power system can be described by using four transfer functions. These four transfer functions are defined in equation (4.15). In the practical use of control systems it is common to specify the closed–loop performance. In our case there are four separated transfer functions, even tough the inputs or outputs are not completely independent. As a consequence of these four transfer functions, the control loop has four controllers as well, four closed–loops. The system is represented in equation (4.18). Thus, since steer–by–wire has only two transfer functions, both of them needs to be controlled by two controllers. For example the steering wheel subsystem has one transfer function on steer–by–wire, but its output — based on the equality — dependens on both the driver's angle and the rack's force. These two external inputs affect only one transfer function, that similarly has two different specified closed–loop performances. This two–control–for–one–process system is shown on Figure 4.9.

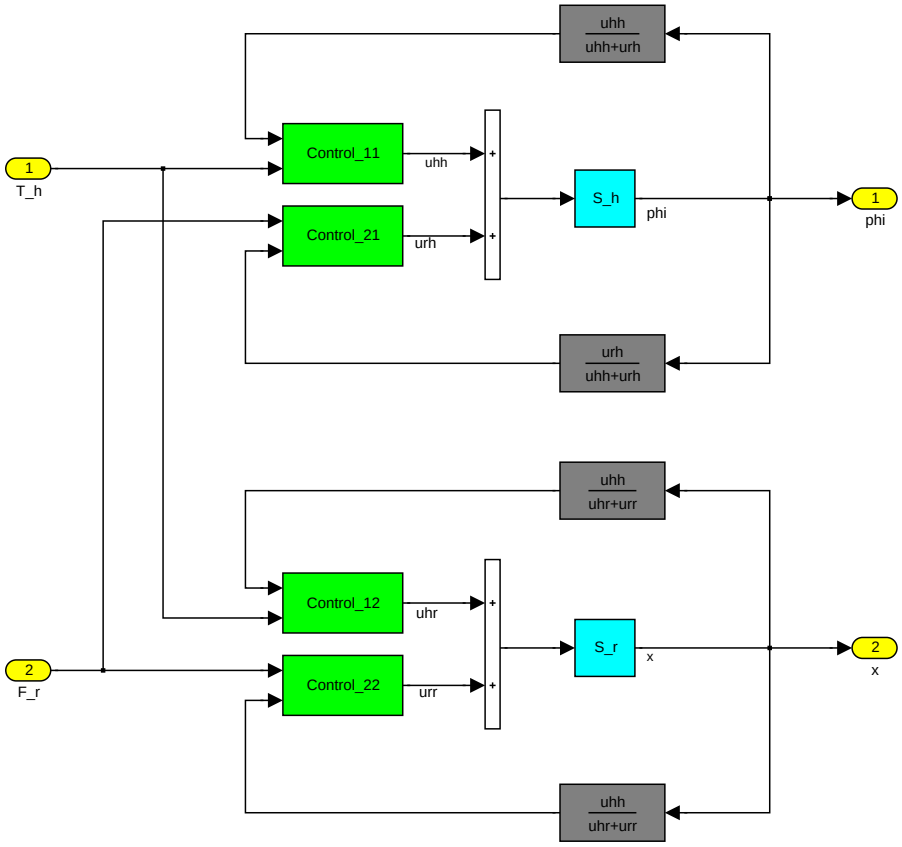

Figure 4.9: The Simulink environment block diagram testing the equality

By examing the closed–loop performance it is necessary to know the effect of

the coherent input. It is possible to share the output value on the basis of the proportions measured on the inputs, using the linear system's superposition ability.

On the other hand it is not possible to measure the values of the external inputs (rack force and driver torque) for counting its weights. This problem might be solved by a *load estimation* [1] for the inputs T_h and F_r. The controller described in section 4.2 does not need numerical information about these inputs. Figure 4.10 shows the block diagram of the MRAC system complemented by the load estimation.

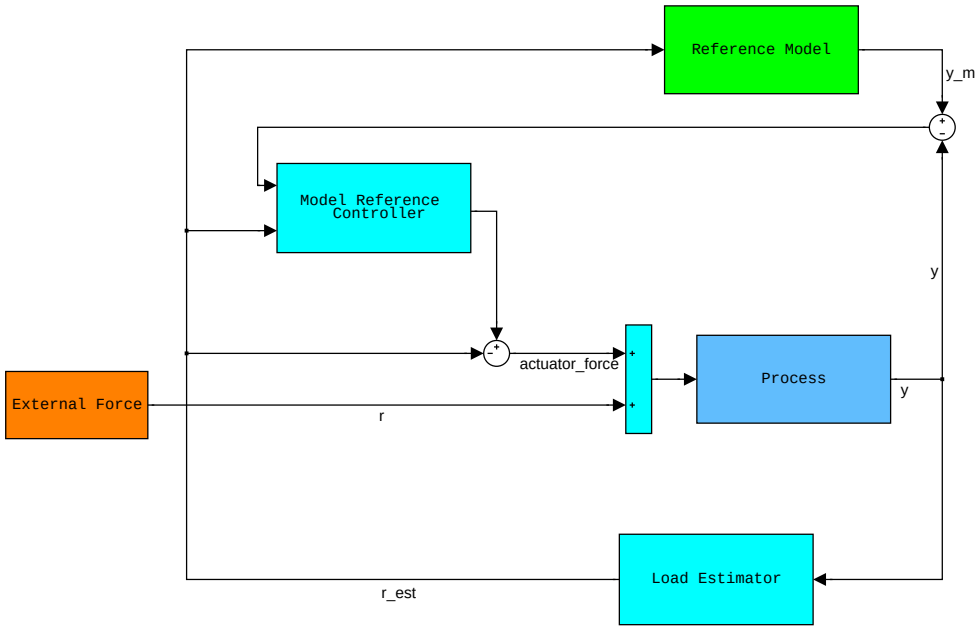

Figure 4.10: The block diagram of the adaptive control with load change

4.3.1 Two–degree–of–freedom controller

This model reference controller bases on a two–degree-of–freedom controller [1]. This controller has a feedback compensator and a feedforward compensator, that means there are two degrees of freedom on designing the closed–loop performance. Another advantage of this controller is that it possibly offers more flexibility than other single cascade compensations.

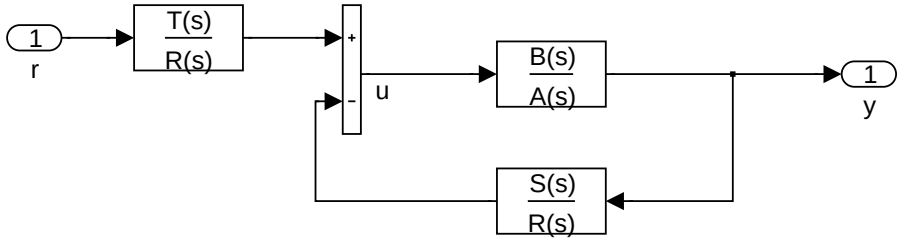

Figure 4.11: The Simulink environment block diagram testing the equality

This controller allows to describe a transfer function B_m/A_m for the closed–loop. This transfer function is called *reference model*, which is the same like the sufficient P_{io} transfer function.

$$W_{closed-loop} = \frac{\frac{T}{R}\frac{B}{A}}{1 + \frac{B}{A}\frac{S}{R}} = \frac{BT}{AR + BS} = \frac{B_m}{A_m} = P_{io} \tag{4.20}$$

Notice that B/A is the controlled system (S_h or S_R), and polynomials R, S and T should be designed during this procedure.

Introducing an observer polynomial A_o equation (4.20) can be written in the following form

$$\frac{BT}{As^l R_1' + BS} = \frac{B_m}{A_m} \cdot \frac{A_o}{A_o}. \tag{4.21}$$

With the neglegances described in section 3.2 the equations (3.24) and (3.27) shows that both S_h and S_R transfer functions have constant numerators. Thus, based on equation (4.21), the zeros of transfer function P_{io} must be among the roots of the polynomial T. Thus, polynomial T is:

$$T = \frac{B_m A_o}{B}, \tag{4.22}$$

Usually integral action control is used which allows to separate the R polynomial — where l is the number of the integrators —

$$R = s^l R_1^{'}, \tag{4.23}$$

and the following condition is given:

$$As^l R_1^{'} + BS = A_m A_o \tag{4.24}$$

A few polynomial order conditions have to be defined for causality.

The polynomial order of a polynomial X is shown by the value of grX.

Different power system transfer functions have different dimensions as it is shown in Table 4.1.

	P_{11} and P_{22}	P_{12} and P_{21}
grA_m	4	4
grB_m	2	0
grA	2	2
grB	0	0

Table 4.1: Polynomial orders of power system and steer–by–wire system

As Table 4.1 shows $grA > grB$. For the controller causality, it is necessary to $grR \geq grS$. Based on these two facts the expression below can be deducted using equation (4.20).

$$gr(AR) = gr(AR + BS) = grB + grA_m + grA_o$$

$$gr(AR) = grA + grB \Rightarrow grR = grB + grA_m + grA_o - grA \tag{4.25}$$

$$grR_1^{'} = grR - grB - l \tag{4.26}$$

The values of grT is achieved using equation (4.22).

$$grT = grB_m + grA_o \tag{4.27}$$

Another assumption for the controller causality is that $grR > grT$. In order to resolve $R_1^{'}$ and S in equation (4.24), the following condition must be realized:

$$grS < grA + l \Rightarrow grS := grA + l - 1 \tag{4.28}$$

Now the $grR \geq grS$ assumption gives the following inequality for the polynomial A_o.

$$grB + grA_m + grA_o - grA \geq grA + l - 1$$

$$grA_o \geq 2grA - grA_m - grB - 1 + l \tag{4.29}$$

The above mentioned integrator might have the effect to cancel the steady state error on the closed–loop. At the power system, all the four transfer functions contain an integrator. Thus, to get the mentioned effect of the integrator the closed–loop should contain an additive one, so $l = 2$ was chosen. Another admissible parameter is the value of grA_o, and the value of its polynomial. As $grA_o \geq 0$ equation (4.29) has no limitation about this value. A value of $grA_o = 2$ was chosen, with the parameters

$$A_o = s + 60. \tag{4.30}$$

It is possible to find a basic difference between polynomials. If the first coefficient is 1 than one can say, it is a monic. The following procedure utilises that the polynomials A, R, A_m and A_o are monics.

The next step is to solve equation (4.24). The solution for this equation provides a solution for polynomials R_1' and S. This equation is a Diophanthine-equation:

$$A_D \cdot X + B_D \cdot Y = C_D \tag{4.31}$$

Where A_D ,B_D C_D is known as follows.

$$A_D = As^l = As \tag{4.32a}$$
$$B_D = B \tag{4.32b}$$
$$C_D = A_m A_o \tag{4.32c}$$

It is now important to view the exact polynomial orders of R_1' and S to solve the Diophanthine-equation. Thus, using equations (4.26) and (4.28), one gets the values:

$$grR_1' = 1 \tag{4.33a}$$
$$grS = 3 \tag{4.33b}$$

	P_{11} and P_{22}	P_{12} and P_{21}
$grR_1^{'}$	1	1
grS	3	3
grR	3	3
grT	3	1

Table 4.2: Polynomial orders of the two–degree-of–freedom controller

Thus, the polynomial orders collected in Table 4.2.

All polynomial orders are known for the Diophanthine-equation, so these polynomials are able to be written in the following form

$$R_1^{'} = 1s + R_1 \tag{4.34a}$$

$$S = S_1 s^3 + S_2 s^2 + S_3 s + S_4 \tag{4.34b}$$

$$A_D = s^5 + A_1 s^4 + A_2 s^3 \tag{4.34c}$$

$$C_D = s^6 + C_1 s^5 + C_2 s^4 + C_3 s^3 + C_4 s^2 + C_5 s + C_6. \tag{4.34d}$$

Over these informations about the Diophanthine-equation, it can be transformed to the following matrix form

$$\underline{C_M} = \underline{\underline{A_M}} \cdot \underline{B_M}.$$

$$\begin{bmatrix} C_1 - A_1 \\ C_2 - A_2 \\ C_3 \\ C_4 \\ C_5 \end{bmatrix} = \begin{bmatrix} 1 & 0 & 0 & 0 & 0 \\ A_1 & B & 0 & 0 & 0 \\ A_2 & 0 & B & 0 & 0 \\ 0 & 0 & 0 & B & 0 \\ 0 & 0 & 0 & 0 & B \end{bmatrix} \cdot \begin{bmatrix} R_1 \\ S_1 \\ S_2 \\ S_3 \\ S_4 \end{bmatrix} \tag{4.35}$$

Based on the fact that A_D is a square–matrix, which can be inverted, so the result vector B_D is got by using the equation

$$\underline{B_M} = \underline{\underline{A_M}}^{-1} \cdot \underline{C_M}. \tag{4.36}$$

Since polynomials S and T are defined above, only the value of R is not known, but it is achieved in

$$\underline{R} = B^{+} \cdot R_1^{'} \cdot s^{l}. \tag{4.37}$$

An easy way to test the designed parameters is when the Bode-plots —the one of the reference transfer function and the other of the closed–loop — are compared. Shown on Figure 4.12.

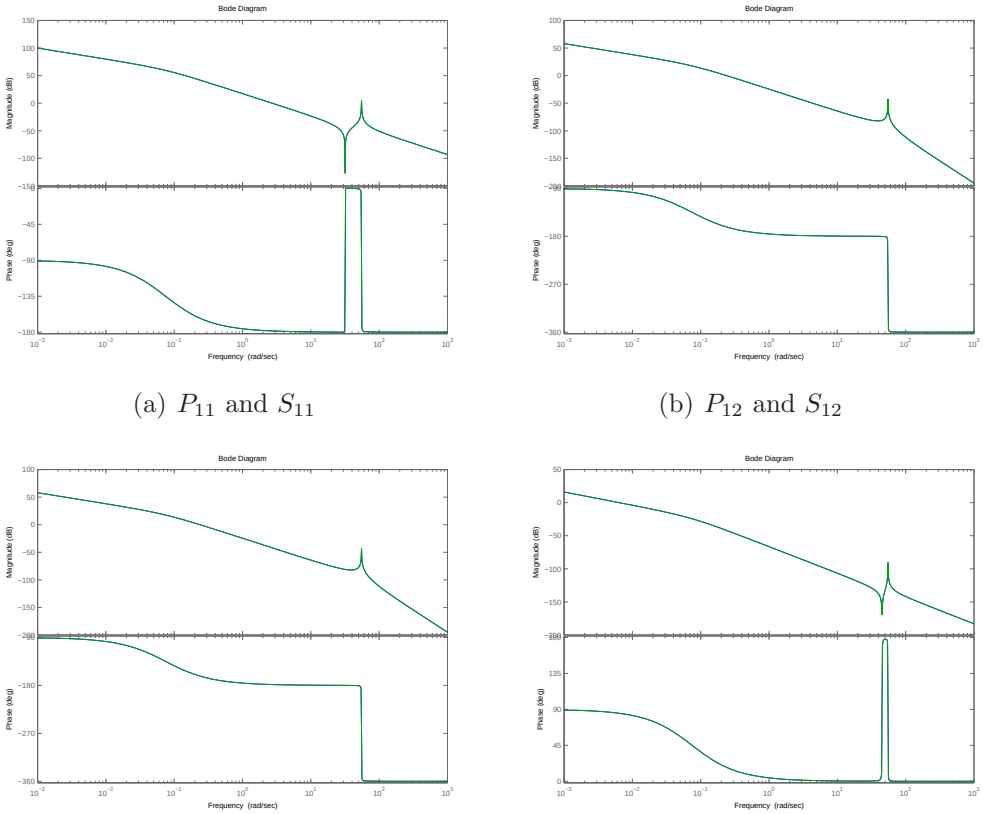

(a) P_{11} and S_{11}

(b) P_{12} and S_{12}

(c) P_{21} and S_{21}

(d) P_{22} and S_{22}

Figure 4.12:
Bode-diagrams of power system's (blue) and steer–by–wire system's with two–degree–of–freedom (green)

In MATLAB Simulink environment it is possible to simulate the system without the *load estimation*, using the real values from the model. The results — are shown in Figure 4.13 — show improvement compared to the controller described in previous section.

It is possible to model disturbances on the input and on the output of the steer–by–wire system, in order to examine their effect on the closed–loop.

In this system the output depends on the signals r, d and e. another disturbance is able to be modeled — the parameters' uncertainty — that can be signed as $W_{uncertainty} = \tilde{B}/\tilde{A}$. The relation is possible to be described in

$$y = \frac{\tilde{B}}{\tilde{A}}\left(\frac{T}{R}r - \frac{S}{R}y + d\right) + e. \tag{4.38}$$

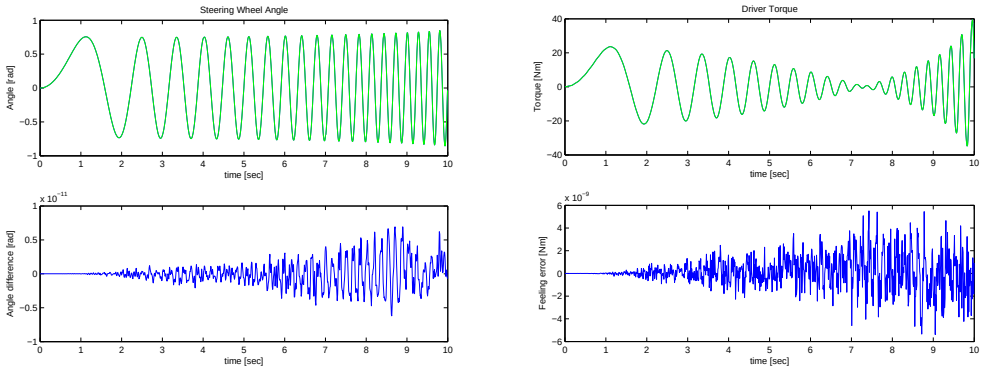

(a) The steering wheel angles

(b) The driver's torques

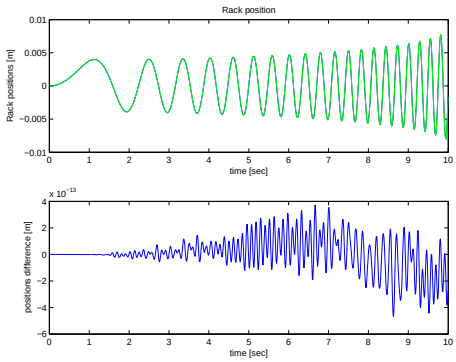

(c) The rack's positions

Figure 4.13:
Compare the derived power system (blue) and the 2DoF controlled steer–by–wire system (green)

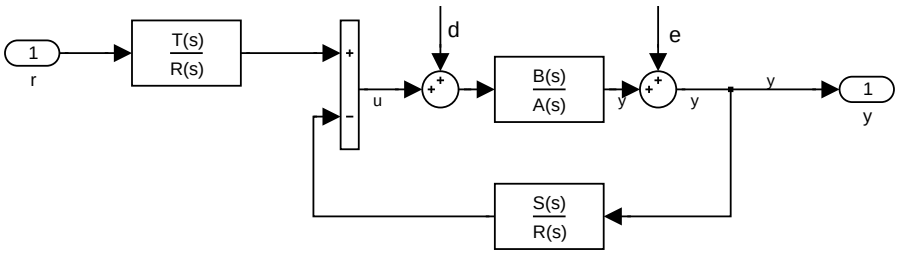

Figure 4.14: Two–degree–of–freedom controller with disturbances

The three additional inputs — r, d and e — have three different transfer functions on the system. These are described as:

$$y = \frac{\tilde{B}T}{\tilde{A}R + \tilde{B}S}r + \frac{\tilde{B}R}{\tilde{A}R + \tilde{B}S}d + \frac{\tilde{A}R}{\tilde{A}R + \tilde{B}S}e. \tag{4.39}$$

Assuming a stable system, the effect of the uncertainties for step signals at time infinity is accomplished by using the formula

$$h_s = y(t \to \infty) = \lim_{s \to 0} \left[s \cdot \frac{y(s)}{s} \right]. \tag{4.40}$$

Hence the closed–loop contains integrators the value of polynomial R at time infinity is $R(s = 0) = 0$.

$$r = 1(t) \Rightarrow y_r(s \to 0) = \frac{T(s \to 0)}{S(s \to 0)} \tag{4.41a}$$

$$d = 1(t) \Rightarrow y_d(s \to 0) = 0 \tag{4.41b}$$

$$e = 1(t) \Rightarrow y_e(s \to 0) = 0 \tag{4.41c}$$

Thus, this controller has the property to compensate the steady state error, and parameter uncertainty. The following figures (Figure 4.15 and 4.16) are illustrating the integrator's effect on uncertain model parameters. As above, at section 4.2, a controller have been planned for the identified system, and another system — with the nominal system parameters increased by 25% — has been used for computing the closed–loop's Bode–diagram (see Figure 4.15), and for running the simulation with.

Bode-diagram on Figure 4.15 shows, that the closed-loop has only a small error in frequency domain. On lower frequencies the difference is smaller, that is caused by the integrator. This effect can be seen on Figure 4.16, too.

On the other hand the closed–loop's stability depends on the roots of the equation

$$\tilde{A}R + \tilde{B}S = 0 \tag{4.42}$$

Thus it depends on the rate of the uncertainties. Note, that the contemplation of the controller using this polynomial method does not promise the stability of the controller. It is possible to reach an unstable controller that is not realisable. Simulating with a growing frequency reference angle, the controller becomes unstable.

As it can be seen by the simulations (for example on Figure 4.16), without assistance force, the driver needs to drive using big torque. This assist force, at this

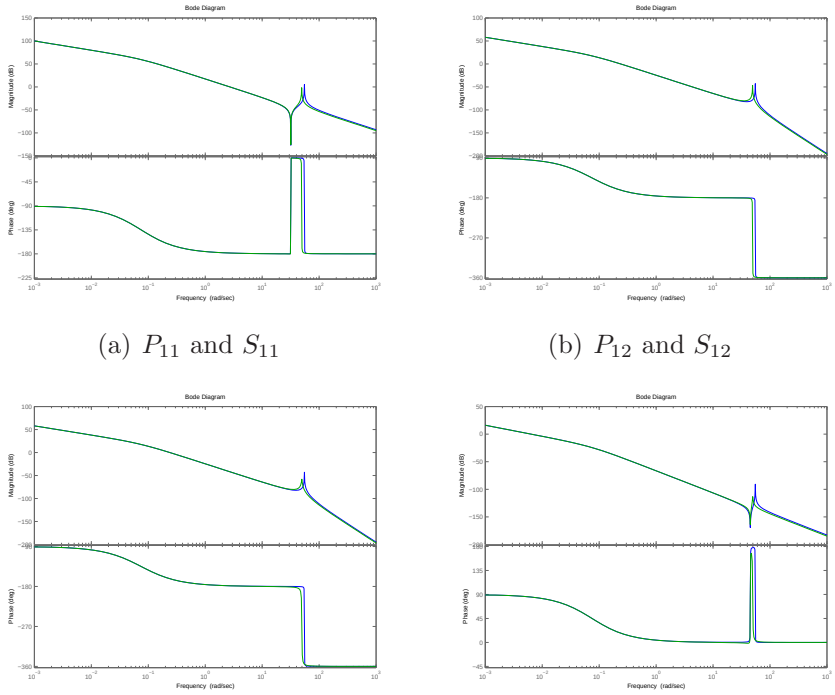

(a) P_{11} and S_{11} (b) P_{12} and S_{12}

(c) P_{21} and S_{21} (d) P_{22} and S_{22}

Figure 4.15:
Bode-diagrams of power system's (blue) and 2DoF controlled steer–by–wire system's (green)

control strategy can not be an arbitrary non–linearity, because the closed–loop must be linear (see equation (4.20)).

There are several other possibilities for this assistance:

- The assist force can be described by a linear function K with driver torque input. This way the transfer function P'_{12} can be defined in the form:

$$P'_{12} = K(s) \cdot P_{12}(s). \tag{4.43}$$

- The assist force is a non–linear function, but its effect on the rack's position must be well known. This effect needs to be reduced from the rack's position, because it is important to close the loop with the feedback value it caused (see Figure 4.9.)

Thus, the two–degree–of–freedom controller is able to make static uncertainties disappear, but changing disturbances possibly make it unstable.

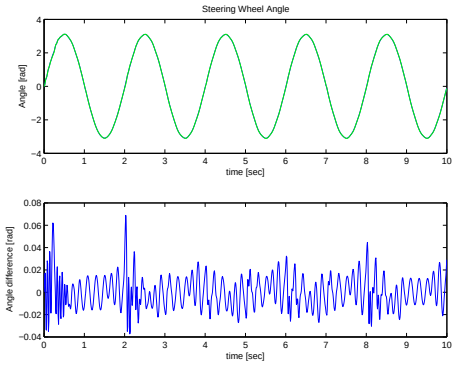

(a) The steering wheel angles

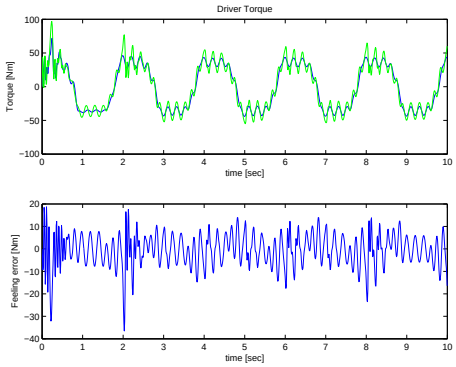

(b) The driver's torques

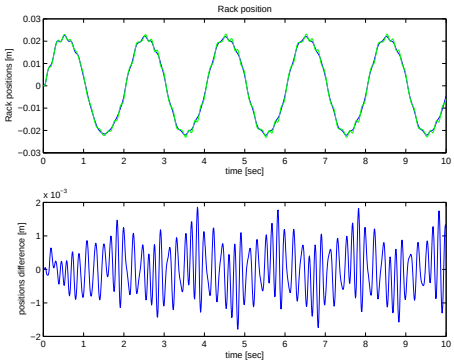

(c) The rack's positions

Figure 4.16:
Compare the power system (blue) and the 2DoF controlled steer–by–wire system (green) with parameters increased by 25%

4.3.2 Model Reference Adaptive Control (MRAC)

The procedure described here is based on [2]. Many dynamic systems to be controlled have both parametric and dynamic uncertainties. Adaptive control is an approach for controlling such systems. Today, techniques from adaptive control are being used to augment many of the existing controllers that have already a proven performance for a certain range of parameters, and adaptation is being used to improve the performance beyond those limits.

A control has been chosen to handle the uncertainties of the steer–by–wire system called model reference adaptive control. This control is based on the above mentioned two–degree–of–freedom controller that has the ability to describe a transfer function for the closed–loop. Thus, it is adjusting the parameters of the polynomial R, T, and S, in order to achieve the reference transfer function. The adaptation law is

$$\frac{d\vartheta}{dt} = \gamma\varphi_{adaptive}e. \tag{4.44}$$

That depends on the gradient of the error e, on the value of the learning rate γ, and on a sort of measured signals $\varphi_{adaptive}$. This adaptation method works for strictly positive real systems.

Definition 1. *A rational transfer function G with real coefficients is positive real if $Re\ G(s) \geq 0$ for $Re\ s \geq 0$. A transfer function G is strictly positive real (SPR) if $G(s-\varepsilon)$ is positive real for some real $\varepsilon > 0$.*

- *The function has no poles in the right half-plane.*
- *$G(s)$ has no poles or zeros on the imaginary axis.*
- *The real part of $G(s)$ is nonnegative along the $i\omega$ axis, that is, $Re\ (G(i\omega)) \geq 0$*

The error is the difference between the required and the current systems' output. Thus, this system requires the reference model's real–time simulation to the control. This simulation requires to know the exact values of the inputs driver's torque and rack's force. Thus, a load estimation needs to be designed into the real loop.

The reference system is $y_m = P_{io}r$. The steer–by–wire system is described with transfer functions S_h and S_R, theirs input u, as it shown in Figure 4.11. Thus, the controller can be written as follows:

$$u = \frac{T}{R}r - \frac{S}{R}y. \tag{4.45}$$

Equation (4.20) can be adjusted to the following form:

$$\begin{aligned} A_o A_m y = (A s^l R_1^{'} + BS)y = R_1^{'}(A s^l y) + BSy = \\ = R_1^{'} s^l (Bu) + BSy = B(Ru + Sy). \end{aligned} \tag{4.46}$$

$$A_o A_m y_m = A_o B_m r = BTr \tag{4.47}$$

Define the error as $e(t) = y_m(t) - y(t)$. Using equations (4.47) and (4.46), this error can be expressed as a function of r, u and y:

$$A_o A_m e = BTr - B(Ru + Sy) \tag{4.48a}$$

$$e = \frac{B}{A_o A_m}(Tr - Ru - Sy) \tag{4.48b}$$

The transfer function $\dfrac{B}{A_o A_m}$ in e is not SPR in all cases, so an *error-filtering* is used.

$$e_f := \frac{Q}{P} e \tag{4.49}$$

Where Q should satisfy:

$$grQ \leq gr(A_o A_m) \tag{4.50a}$$

$$\frac{Q}{A_o A_m} \rightarrow SPR \tag{4.50b}$$

It is an easy way to design Q for $A_o A_m$ if $Q = A_o A_m$. Polynomial $P = P_1 P_2$. Where $grP_1 > grP_2$, $grP_2 = grR = k$, $grS = l$ and $grT = m$, and P_2 is monic. It is possible to write R/P in the following form:

$$\frac{R}{P} = \frac{R - P_2 + P_2}{P_1 P_2} = \frac{1}{P_1} + \frac{R - P_2}{P} \tag{4.51}$$

Now equation (4.49) can be converted into the form:

$$e_f = \frac{Q}{P} e = \frac{BQ}{A_o A_m} \left(-\frac{u}{P_1} - \frac{R - P_2}{P} u - \frac{S}{P} + \frac{T}{P} r \right) \tag{4.52}$$

By parameterizing the filtered error, two vectors are possible to be defined.

$$\vartheta_0 := (r_1^{'}, r_2^{'}, \ldots, r_k^{'}, s_0, s_1, \ldots, s_l, t_0, t_1, \ldots, t_m)^T \tag{4.53}$$

$$\varphi_{adaptive} := \left(-\frac{p^{k-1}}{P(p)}u, \ldots, -\frac{1}{P(p)}u, -\frac{p^l}{P(p)}y, \ldots, -\frac{1}{P(p)}y, \frac{p^m}{P(p)}r, \ldots, \frac{1}{P(p)}r \right) \tag{4.54}$$

Where $p = \dfrac{d}{dt}$ is a differential operator. This simplifies the (4.52) expression.

$$e_f = \frac{BQ}{A_o A_m} \left(-\frac{u}{P_1} + \varphi^T_{adaptive}\vartheta_0 \right) \tag{4.55}$$

The control law is chosen as $u := \vartheta^T(P_1\varphi_{adaptive})$ that is realizable. Thus, one can make further expression for filtered error.

$$\begin{aligned} e_f &= \frac{BQ}{A_o A_m} \left(\varphi^T_{adaptive}\vartheta - \frac{1}{P_1}\vartheta^T(P_1\varphi_{adaptive}) \right) = \\ &= \frac{BQ}{A_o A_m}\varphi^T_{adaptive}(\vartheta_0 - \vartheta) - \frac{BQ}{A_o A_m} \left(\frac{1}{P_1}u - \varphi^T_{adaptive}\vartheta \right) \end{aligned} \tag{4.56}$$

The error augmentation is $\eta = \left(\dfrac{1}{P_1}u - \varphi^T_{adaptive}\vartheta \right)$. The augmented error is ε, described as:

$$\varepsilon := e_f + \frac{BQ}{A_o A_m}\eta \tag{4.57}$$

It is possible to define variables φ_f and u_f filtered signals.

$$\varphi_f = \frac{Q}{A_o A_m}\varphi_{adaptive} \tag{4.58a}$$

$$u_f = \frac{Q}{A_o A_m P_1}u \tag{4.58b}$$

The parameter adaptation law should be chosen to minimize the expression:

$$V = \frac{1}{2}\varepsilon_p^2 \to min \tag{4.59}$$

Where $\varepsilon_p = e_f - \hat{e}_f = e_f - \hat{B}(\varphi_f^T\vartheta - u_f)$ is the error of the prediction.

$$\frac{d\vartheta}{dt} = \gamma\varphi_f\varepsilon_p \tag{4.60a}$$

$$\frac{dB}{dt} = \gamma_0 \left(\varphi_f^T\hat{\vartheta} - u_f \right) \varepsilon_p \tag{4.60b}$$

The block diagram of the MRAC system is can seen on Figure (4.17).

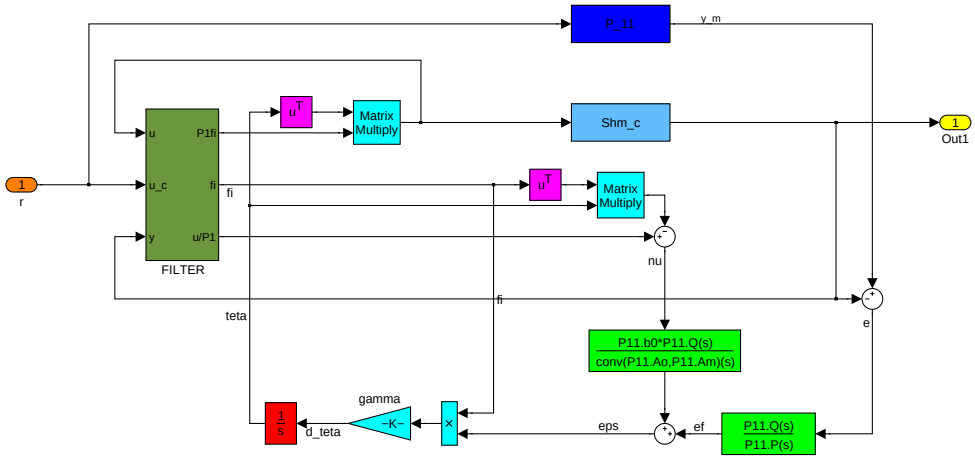

Figure 4.17: Realization of the MRAC in Simulink environment

For the realization of this controller it is necessary to get the signals $P_1\varphi_{adaptive}$, $\varphi_{adaptive}$ and $\dfrac{u}{P_1}$. These signals can be derived using r, u and y signals. The polynomial form of P_1 and P_2 is:

$$P_1 = p^n + \alpha_1 p^{n-1} + \cdots + \alpha_{n-1}p + \alpha_n \tag{4.61a}$$

$$P_2 = p^k + \beta_1 p^{k-1} + \cdots + \beta_{k-1}p + \beta_k \tag{4.61b}$$

Thus, the above mentioned problem can be solved as a special case of the following one:

$$P_1\varphi_{u_*} = (x_1, \ldots, x_k)^T,\ x_1 = \frac{p^{k-1}}{P_2}u_*, \ldots, x_k = \frac{1}{P_2}u_* \tag{4.62}$$

The generic solution requires two state–equations, and the results are going to implemented as $(x, z)_{u_*}$. These two differential equations in matrix form have the polynomial companion matrix of the polynomials:

$$\begin{bmatrix} \dot{x_1} \\ \dot{x_2} \\ \dot{x_3} \\ \vdots \\ \dot{x_k} \end{bmatrix} = \begin{bmatrix} -\beta_1 & -\beta_2 & \dots & -\beta_{k-1} & -\beta_k \\ 1 & 0 & \dots & 0 & 0 \\ 0 & 1 & \dots & 0 & 0 \\ \vdots & & \ddots & \vdots & \\ 0 & 0 & \dots & 1 & 0 \end{bmatrix} \begin{bmatrix} x_1 \\ x_2 \\ x_3 \\ \vdots \\ x_k \end{bmatrix} + \begin{bmatrix} 1 \\ 0 \\ 0 \\ \vdots \\ 0 \end{bmatrix} u_* \tag{4.63a}$$

$$\begin{bmatrix} \dot{z_1} \\ \dot{z_2} \\ \dot{z_3} \\ \vdots \\ \dot{z_n} \end{bmatrix} = \begin{bmatrix} -\alpha_1 & -\alpha_2 & \dots & -\alpha_{n-1} & -\alpha_n \\ 1 & 0 & \dots & 0 & 0 \\ 0 & 1 & \dots & 0 & 0 \\ \vdots & 0 & \ddots & \vdots & 0 \\ 0 & 0 & \dots & 1 & 0 \end{bmatrix} \begin{bmatrix} z_1 \\ z_2 \\ z_3 \\ \vdots \\ z_n \end{bmatrix} + \begin{bmatrix} 1 \\ 0 \\ 0 \\ \vdots \\ 0 \end{bmatrix} x_k \tag{4.63b}$$

One can see that the second state–space representation has the input equal to the first state–space description's last state, so it is solvable in case the first state–equation is solved. The required signs are possible to be yielded using the following equations, where the value of $dim\varphi_{u_*}$ is for example k for input u:

$$\varphi_{u_*} = \left(z_{n-(dim\varphi_{u_*}-1)}, \dots, z_n\right)^T \tag{4.64a}$$

$$P_1\varphi_{u_*} = \left(x_{k-(dim\varphi_{u_*}-1)}, \dots, x_k\right)^T \tag{4.64b}$$

$$\frac{u_*}{P_1} = z_{n-k} + \beta_1 z_{n-k+1} + \dots + \beta_k z_n \tag{4.64c}$$

The final values of this signals are the interlink of the three $(z,x)_{-u}$, $(z,x)_{-y}$ and $(z,x)_r$ blocks.

The Simulink environment based realization of the filter is can be seen on Figure 4.18.

Let us now realize the MRAC controller. Based on the two–degree-of–freedom controller, the polynomial orders of polyinomials S, T and R are known, and the vector ϑ_0 is also known. The adjustable parameter quantities can be seen in Table 4.3. Then, the task is to realize the filter. As it can be seen, all state-space blocks x have $grR = k = 3$ pieces of inner states. The signal $P_1\varphi_{u_*}$ has $dim\varphi_{u_*}$ dimensions. Its quantities are countable from equation (4.54), and can be seen on Table 4.4.

The controller can not be realized using these parameters. The assumption of the realization is to enhance the states of filter x. This value depends on grP_2. As grP_2 is equal to grR, the polynomial order of R should be increased at least with one order, in the view that grS and grT values need to be less than this increased

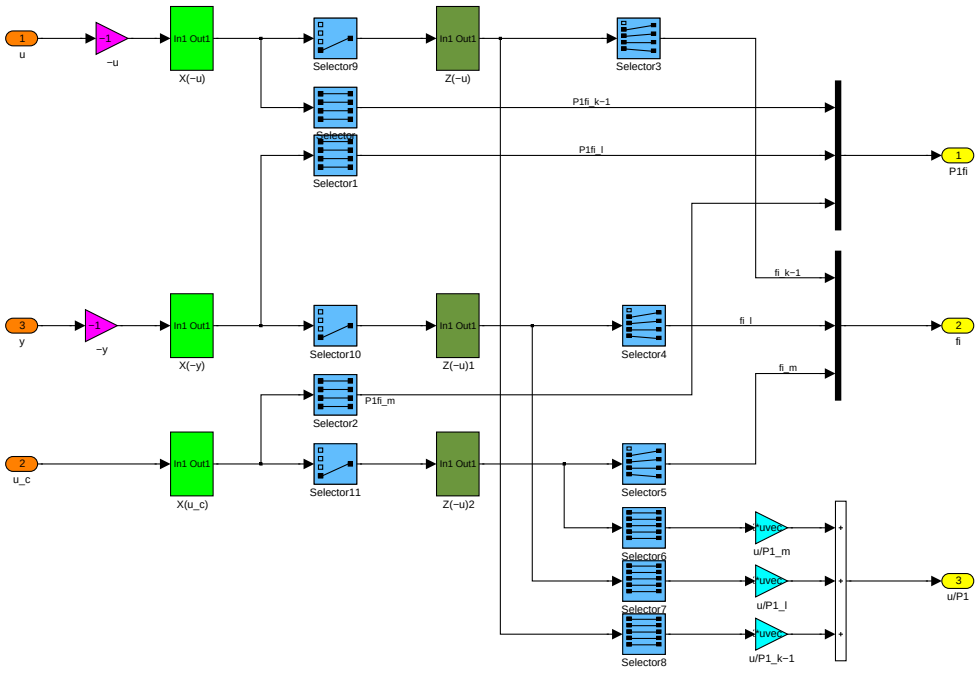

Figure 4.18: Realization of the filter block in Simulink environment

	P_{11} and P_{22}	P_{12} and P_{21}
R	3	3
S	4	4
T	4	2

Table 4.3: Number of adjustable parameters depends on the reference model

value of grR. The only way to reach this — based on equations (4.25), (4.27) and (4.28) — is to step up the polynomial order of A_m.

The polynomial A_m is the denumerator part of the desired transfer function, P_{io}. If it is changing, the power system's parameters are changing, but the aim is to create a controller that assures the same road feel like the power system. It is possible to create negligible pole on the transfer functions, that raises the value of grA_m, but makes a minimal change on the frequency domain. Thus, during the design procedure, the transfer functions P_{io} are modified with an additive pole:

$$P_{ioDesign} = P_{io} \cdot \frac{2\pi f}{s + 2\pi f} \tag{4.65}$$

The value $f = 100Hz$ was chosen, because this frequency is over the driver's detection limit, and force ability.

The effect of this change can be shown by plotting the bode-diagram of P_{io} and

	P_{11} and P_{22}	P_{12} and P_{21}
r	4	2
u	3	3
y	4	4

Table 4.4: The values of $dim\varphi_{u_*}$

$P_{ioDesign}$, see Figure 4.19.

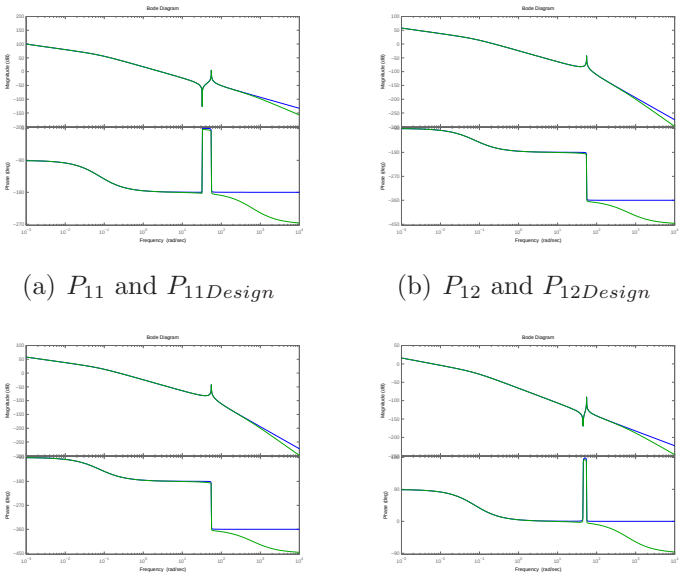

(a) P_{11} and $P_{11Design}$ (b) P_{12} and $P_{12Design}$

(c) P_{21} and $P_{21Design}$ (d) P_{22} and $P_{22Design}$

Figure 4.19: Bode-diagrams P_{io} (blue) and $P_{ioDesign}(green)$

Using this power system, the polynomial orders became the value that can be seen on Table 4.5. The quantity of adjustable parameters and the value of dimφ_{u_*} can be seen on Table 4.6. One can see that the controller is realizable now referring to the polynomial orders.

The model reference adaptive controller described above was interpreted on the identified transfer functions, S_h and S_R, with the reference models P_{io}. As mentioned, the steer–by–wire system's transfer functions have two controllers, two reference models. Thus, S_h has the reference models P_{11} and P_{21}. Similarly, S_R has the reference models P_{22} and P_{12}. These four model reference controllers were represented in MATLAB Simulink environment. The result on the nominal steer–by–wire system can be seen on Figure 4.20. To view the effects of the parameters' uncertainty a simulation was run with changed steer–by–wire parameters. The parameters were increased by 25% — (see Figure 4.21) — but the controller had the ability to

	P_{11} and P_{22}	P_{12} and P_{21}
grA_m	5	5
grB_m	2	0
grA	2	2
grB	0	0
grR	4	4
grS	3	3
grT	3	1

Table 4.5: Polynomial orders with reference models $P_{ioDesign}$

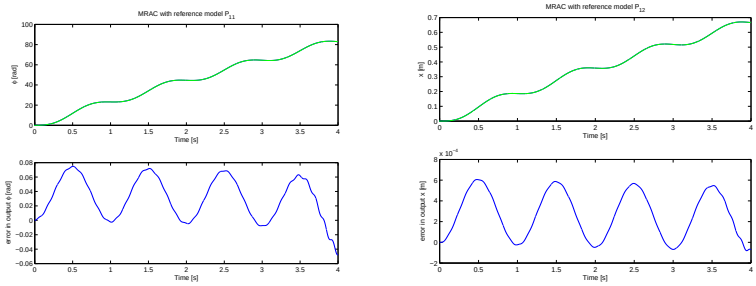

(a) MRAC with reference P_{11}

(b) MRAC with reference P_{12}

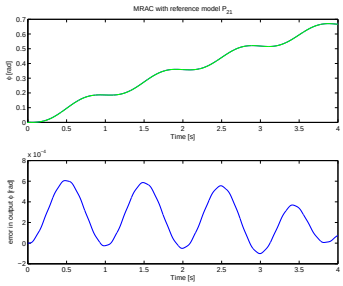

(c) MRAC with reference P_{21}

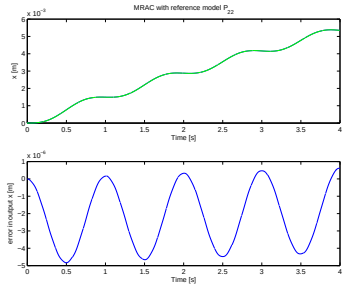

(d) MRAC with reference P_{22}

Figure 4.20:
Implemented MRAC (blue) on the four transfer function (green) with nominal system

suppress the steady state error.

The model reference adaptive controller has not been managed yet. During the simulation the controller becomes instable. This effect is possibly caused by an additive signal that is detectable on the controller output. This signal can be viewed on the error signals on Figures 4.20 and 4.21, and has a frequency that depends on the input signal. Our future task is to find the origin of this additive signal.

(a) Values of adjustable parameters

	P_{11} and P_{22}	P_{12} and P_{21}
R	4	4
S	4	4
T	4	2

(b) Values of $dim\varphi_{u_*}$

	P_{11} and P_{22}	P_{12} and P_{21}
u	4	4
y	4	4
r	4	2

Table 4.6: The value of adjustable variables and $dim\varphi_{u_*}$

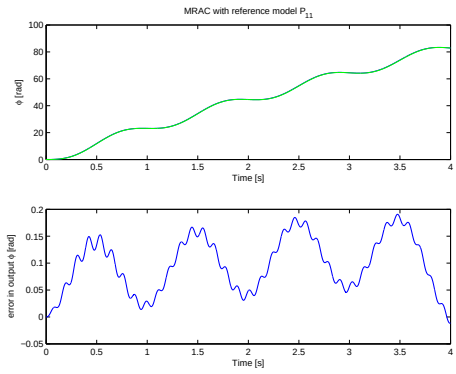

(a) MRAC with reference P_{11}

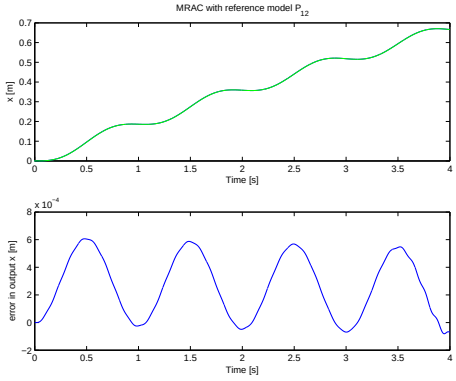

(b) MRAC with reference P_{12}

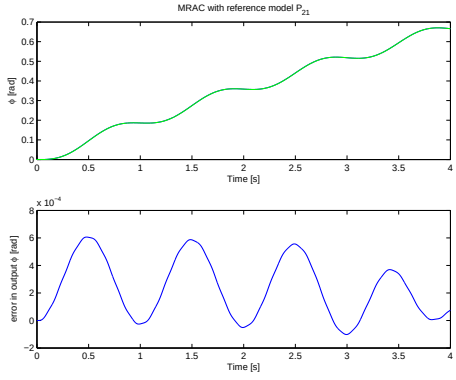

(c) MRAC with reference P_{21}

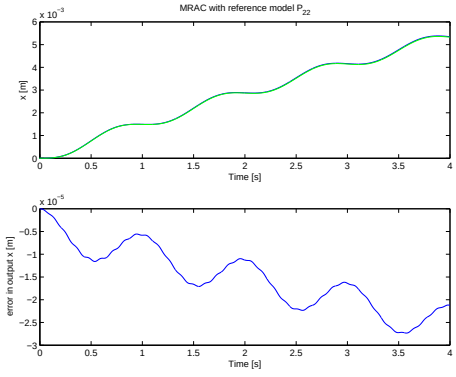

(d) MRAC with reference P_{22}

Figure 4.21:
Implemented MRAC (blue) on the four transfer function (green) with steer–by–wire system parameters increased by 25%

Chapter 5

Conclusion

This Diploma investigated methods for ensuring the *road feel* with a force feedback controller. The constructed model of the steer–by–wire system based on ARMAX identification method. To ensure the *road feel* the properties of a conventional steering system was copied by the controller. The structure of this controller is the main concept of this thesis.

The first step in design procedure was implemented with a concept of [3]. This method established the equality of positions and forces on linear systems. The performance of this equality is reduced by the parameter uncertainties, thus a two–degree–of–freedom controller — that proved to be robust in other applications — performed on the system.

The controller was implemented in model reference control architecture, that proposed the *road feel* equivalence. In order to improve the performance, the controller parameters were tuned adaptively (Model Reference Adaptive Controller — MRAC). This provides a good stability for uncertainties, and has the ability to copy the attributes of a conventional steering system. A further task is to fit this controller to the steer–by–wire system, but we expect a good stability and model following from this control strategy.

There are several other questions that should be solved in the future. The implementation of these controllers into a car might require a better identification with targeted measurements. In fact the controllers based on the two–degree–of–freedom controller need a load estimator, to be planned for real application.

We offered three controller on steer–by–wire system. All of them are able to copy the properties of a conventional steering system. Their effectiveness depends on the information we know about the steering system, and on the system's uncertainties.

Chapter 6

Appendix

6.1 Notations of variables and parameters

Notation	Description	Unit
Θ	Equivalent inertia reduced on steering wheel subsystem	$kg \cdot m^2$
φ	Angle of steering wheel	rad
T_h	Driver torque	Nm
τ_{act_h}	Torque of the steering wheel actuator	Nm
T_v	Torque of viscous friction on steering wheel subsystem	Nm
T_c	Torque of Coulomb–friction on steering wheel subsystem	Nm
T_b	Torque of spring on steering wheel subsystem	Nm
M	Equivalent mass on road wheel subsystem	kg
x	Position of the rack	m
F_r	Rack force	N
$F_{act_{Rck}}$	Force of the road wheel actuator	N
F_v	Force of viscous friction on road wheel subsystem	N
F_c	Force of Coulomb–friction on road wheel subsystem	N
F_b	Force of spring on road wheel subsystem	N
i_s	Transmission of ball–screw drive	m/rad

Table 6.1: Notations I.

Notation	Description	Unit
Θ_{Rck}	Equivalent inertia reduced on road wheel subsystem	$kg \cdot m^2$
φ_{Rck}	Angle of road wheel actuator	rad
$T_{h_{Rck}}$	Rack torque	Nm
τ_{Rck}	Torque of the road wheel actuator	Nm
T_{vRck}	Torque of viscous friction on road wheel subsystem	Nm
T_{cRck}	Torque of Coulomb–friction on road wheel subsystem	Nm
T_{bRck}	Torque of spring on road wheel subsystem	Nm
K_{Stw}	Viscous friction coefficient on steering wheel subsystem	$N \cdot s/rad$
K_{cStw}	Coulomb–friction coefficient on steering wheel subsystem	Nm
B_{Stw}	Spring coefficient on steering wheel subsystem	Nm
K_{Rck}	Viscous friction coefficient on road wheel (round)	$N \cdot s/rad$
K_{cRck}	Coulomb–friction coefficient on road wheel (round)	Nm
B_{Rck}	Spring coefficient on road wheel (round)	Nm
K_{xRck}	Viscous friction coefficient on road wheel (direct)	$N \cdot s/m$
K_{xcRck}	Coulomb–friction coefficient on road wheel (direct)	N
B_{xRck}	Spring coefficient on road wheel (direct)	N
T_{InStw}	Equivalent torque of external forces on steering wheel	Nm
T_{InRck}	Equivalent torque of external forces on road wheel	Nm
i_P	Transmission constant between rack and steering column	m/rad
φ_{PS}	Steering wheel angle on the power system	rad
x_{rPS}	Position of the rack on the power system	m

Table 6.2: Notations II.

Bibliography

[1] **Lantos, Béla** *Irányítási rendszerek elmélete és tervezése I.*
Akadémiai Kiadó, Budapest (2001)

[2] **Lantos, Béla** *Irányítási rendszerek elmélete és tervezése II.*
Akadémiai Kiadó, Budapest (2003)

[3] **Dirk Odenthal, Tilman Bünte, Heinz-Dieter Heitzer, Christoph Eicker** *How to make Steer-by-Wire feel like steering*
15th Triennial World Congress, Barcelona, Spain (2002)

[4] **MATLAB** *Reference Manual* The MathWorks, Inc., (2001)

[5] **Ljung, Lennart** *System Identification — Theory for the User, Second Edition*
1999 by Prentice Hall PTR

[6] **Ljung, Lennart** *System Identification Toolbox — For Use with MATLAB*
1997 by The MathWorks, Inc.